Icarus 370 (2021) 114685

Contents lists available at ScienceDirect

Icarus

journal homepage: www.elsevier.com/locate/icarus

Research Paper

Mars' atmospheric neon suggests volatile-rich primitive mantle

Hiroyuki Kurokawa [a,*], Yayoi N. Miura [b], Seiji Sugita [c], Yuichiro Cho [c], François Leblanc [d], Naoki Terada [e], Hiromu Nakagawa [e]

[a] Earth-Life Science Institute, Tokyo Institute of Technology, Japan
[b] Earthquake Research Institute, The University of Tokyo, Japan
[c] The University of Tokyo, Japan
[d] LATMOS/CNRS, Sorbonne Université, UVSQ, France
[e] Tohoku University, Japan

ARTICLE INFO

Keywords:
Atmospheres
Composition
Interiors
Mars
Planetary formation
Volcanism

ABSTRACT

Martian atmospheric neon (Ne) has been detected by Viking and also found as trapped gas in Martian meteorites, though its abundance and isotopic composition have not been well determined. Because the timescale of Ne loss via atmospheric escape estimated from recent measurements with MAVEN is short (0.6–1×10^8 years), the abundance and isotope composition of Martian atmospheric Ne reflect recent atmospheric gas supply mostly from volcanic degassing. Thus, it can serve as a probe for the volatile content of the interior. Here we show that the tentatively-informed atmospheric Ne abundance suggests recent active volcanism and the mantle being richer in Ne than Earth's mantle today by more than a factor of 5–80. The estimated mantle Ne abundance requires efficient solar nebular gas capture or accretion of Ne-rich materials such as solar-wind-implanted dust in the planet formation stage, both of which provide important constraints on the abundance of other volatile elements in the interior and the accretion history of Mars. More precise determination of atmospheric Ne abundance and isotopic composition by in situ analysis or Mars sample return is crucial for distinguishing the possible origins of Ne.

1. Introduction

Planetary interiors record their formation history and influence surface environments through volcanic and tectonic activities. The potentially large volatile content of the mantle is thought to have controlled the climate evolution of early Mars through volcanic supply of atmospheric gases and water (e.g., Craddock and Greeley, 2009; Halevy et al., 2007; Tian et al., 2010; Sholes et al., 2017; Ramirez et al., 2014; Wordsworth et al., 2017). Thanks to exploration missions, the surface environment of Mars and its evolution have been enormously studied. In contrast, its interior is less understood. Given the current surface environment being highly modified by exogenous (impacts and atmospheric escape) and endogenous (volcanic degassing) processes through 4.5 billion years evolution (e.g., Melosh and Vickery, 1989; Jakosky et al., 1994; Pepin, 1991, 1994; Terada et al., 2009; Kurokawa et al., 2014, 2016, 2018; Sakuraba et al., 2019), understanding its interior, which can still possess primitive information, is crucial to unveil the accretion and differentiation history.

Noble gases are chemically inert, and thus useful to study both the origins of planetary volatile elements and atmospheric evolution (e.g., Lammer et al., 2020). The Viking landers detected Martian atmospheric neon (Ne), argon (Ar), krypton (Kr), and xenon (Xe) (Owen et al., 1977). The measured noble gas abundance was consistent with trapped gas in the Antarctic meteorite Elephant Moraine (EETA) 79001, which confirmed Martian origin of the meteorite (Pepin, 1985). Isotopic compositions of Ar, Kr, and Xe in the Martian atmosphere have been measured in situ by Viking and Curiosity (Atreya et al., 2013; Conrad et al., 2016) and recovered from Martian meteorites (Smith et al., 2020, and references therein). Those heavy noble gas isotopes have been used to constrain atmospheric evolution in the distant past (>1 Ga, Pepin, 1991, 1994; Slipski and Jakosky, 2016; Jakosky et al., 2017; Kurokawa et al., 2018). Helium (He) has been found neither in situ nor from trapped gas in Martian meteorites, likely due to its low abundance (Krasnopolsky and Gladstone, 2005; Smith et al., 2020). Ne isotope ratio ($^{20}Ne/^{22}Ne$) has been recovered from trapped gas in Martian meteorites, yet it has not reached consensus (Swindle et al., 1986; Wiens et al., 1986; Garrison and Bogard, 1998; Park and Nagao, 2006; Park et al., 2017; Smith et al., 2020). Although no in situ measurement is available so far, the determination of Ne isotopes by a future mission has been proposed (Miura et al., 2020).

* Corresponding author.
E-mail address: hiro.kurokawa@elsi.jp (H. Kurokawa).

https://doi.org/10.1016/j.icarus.2021.114685
Received 30 April 2021; Received in revised form 16 August 2021; Accepted 25 August 2021
Available online 4 September 2021

Here we show that Martian atmospheric Ne is a powerful probe for the volatile content of its interior and the planet formation history. Section 2 presents the balance between loss and supply of atmospheric Ne and shows the estimate of volcanic degassing flux and mantle Ne abundance. Section 3 presents models for Ne trapping into the mantle in the magma ocean stage to estimate the amount of Ne required in Mars formation stage. Section 4 presents the possible origins of Martian Ne: solar nebula gas, solar-wind-implanted dust, and chondritic materials. Section 5 discuss the requirements for precise determination of Ne abundance and isotopic composition by future missions, constraints from other volatile elements, and the comparison to Earth. We conclude in Section 6.

2. Loss and supply of atmospheric Ne on current Mars

2.1. Current knowledge on Ne abundance and isotope ratio

In situ measurement data of Ne abundance were only reported from Viking mission. Viking mass spectrometers detected $m/e = 22$ (where m and e are the mass and charge numbers) signal and extraction of $^{44}CO_2^{++}$ component derived Martian atmospheric ^{22}Ne abundance to be 0.25 ppm (Owen et al., 1977). Assuming $^{20}Ne/^{22}Ne = 10 \pm 3$ and including the other uncertainties, ^{20}Ne abundance was estimated to be $2.5^{+3.5}_{-1.5}$ ppm (Owen et al., 1977). The abundances of Ne relative to other noble gases recovered from Viking (Owen et al., 1977) and Martian meteorite (Pepin, 1985) are consistent with each other, supporting the validity of the estimates.

Ne isotope ratio of the Martian atmosphere has been reported as an endmember of trapped gas in Martian meteorites. $^{20}Ne/^{22}Ne$ ratios of 10.1 ± 0.7 (Wiens et al., 1986) and 10.6 ± 0.6 (Swindle et al., 1986) have been reported from the analysis of EETA 79001. In contrast, lower values, $^{20}Ne/^{22}Ne = 7$ (Garrison and Bogard, 1998) and 7.3 ± 0.2 (Park and Nagao, 2006; Park et al., 2017) have been also reported from the Yamato (Y) 793605 meteorite and from Dhofar 378 and Northwest Africa 7034, respectively.

While a non-cosmogenic endmember of Ne in Martian meteorites is widely thought to originate from the Martian atmosphere (e.g., Smith et al., 2020), Martian meteorites potentially contain Ne from the Martian interior as another endmember (Mohapatra et al., 2009), as proposed for Ar and Xe (Ott, 1988; Mathew and Marti, 2001; Swindle, 2002; Schwenzer et al., 2007; Filiberto et al., 2016). However, both the isotopic ratio and abundance of potentially mantle-originated Ne are not well established. The dominance of cosmogenic Ne in Martian meteorite samples makes it difficult to understand the origins of trapped Ne components (e.g., Smith et al., 2020).

Though more precise determination is desired, some important conclusions can be derived from the reported values of Martian atmospheric Ne abundance and $^{20}Ne/^{22}Ne$ ratio as below.

2.2. Atmospheric escape

The Martian atmosphere is being continuously lost by atmospheric escape processes (e.g., Jakosky et al., 2018). Noble gases including Ne are removed chiefly by a process called sputtering (Fig. 1): ejection of neutral atoms and molecules from near the exobase via collisions with pickup ions accelerated by the solar wind magnetic field (Luhmann and Kozyra, 1991; Luhmann et al., 1992). As both Ne and Ar are removed by sputtering, we estimate the loss rate of Ne by relating the loss rate with that of Ar (4.9×10^{22} s^{-1}) derived with a recent 3D simulation (Leblanc et al., 2018) which was validated by exospheric observations with The Mars Atmosphere and Volatile Evolution (MAVEN) spacecraft (Leblanc et al., 2019). The relation of sputtering loss rates of two species i, j denoted by $F_{i,\mathrm{sp}}$, $F_{j,\mathrm{sp}}$ can be well approximated by (Johnson et al., 2000; Leblanc et al., 2012),

$$\frac{F_{i,\mathrm{sp}}}{F_{\mathrm{j,sp}}} = \frac{Y_i}{Y_j} = \left(\frac{x_i}{x_j}\right)_{\mathrm{exo}} \frac{U_{\mathrm{es},j}}{U_{\mathrm{es},i}} = R_{\mathrm{diff},i/j}\left(\frac{x_i}{x_j}\right)_{\mathrm{homo}} \frac{U_{\mathrm{es},j}}{U_{\mathrm{es},i}}, \quad (1)$$

where Y_i is the sputtering yield (the number of particles removed per incident ion), x_i is the molar fraction where the subscripts homo and exo denote the homopause and exobase, $U_{\mathrm{es},i}$ is the escape energy, and $R_{\mathrm{diff},i/j}$ is the fractionation factor by diffusive separation between the homopause and exobase (i.e., the difference in the scale heights above the homopause), respectively. The diffusive separation factor is given by,

$$R_{\mathrm{diff},i/j} = \exp\left(-\frac{\Delta m_{i,j} g \Delta z}{k_{\mathrm{B}} T}\right) \simeq \exp\left[-0.446\left(\frac{\Delta z}{1\ \mathrm{km}}\right)\left(\frac{T}{1\ \mathrm{K}}\right)^{-1}\left(\frac{\Delta m_{i,j}}{1\ \mathrm{amu}}\right)\right], \quad (2)$$

where k_{B} is the Boltzmann constant, g is the gravitational acceleration, Δz is the distance between the homopause and exobase, T is the temperature, and $\Delta m_{i,j}$ is the mass difference between two species. From Eq. (1), the lifetime of species i against sputtering loss, τ_i, is given by,

$$\frac{\tau_{i,\mathrm{sp}}}{\tau_{j,\mathrm{sp}}} = \frac{U_{\mathrm{es},i}}{U_{\mathrm{es},j}} R^{-1}_{\mathrm{diff},i/j}. \quad (3)$$

We use Eq. (3) to relate the lifetime of Ne and other noble gases to that of Ar, which is estimated to be 4×10^9 years using the sputtering rate mentioned above. Importantly, the lifetime of minor species other than the dominant molecule CO_2 is independent from the abundance in atmosphere. This is because the loss rates of minor species are proportional to their abundances, and thus the dependence of lifetime on the abundance cancels out.

The isotopic fractionation factor of sputtering is also given by $R_{\mathrm{diff},i/j}$, as the difference in yields is expected to be small. In a steady state where the sputtering loss and supply is balanced, The isotope ratios of the atmosphere and the source are related by (Jakosky et al., 1994; Kurokawa et al., 2018),

$$\left(\frac{^{20}\mathrm{Ne}}{^{22}\mathrm{Ne}}\right)_{\mathrm{source}} = R_{\mathrm{diff},^{20}\mathrm{Ne}/^{22}\mathrm{Ne}} \cdot \left(\frac{^{20}\mathrm{Ne}}{^{22}\mathrm{Ne}}\right)_{\mathrm{atm}}. \quad (4)$$

Eq. (4) is used later in Section 4 to discuss the origins of Martian Ne.

A comparison of Ne lifetime to that of atmospheric carbon (C) provides some insights into its behavior. A model combined to MAVEN's observations of precipitating ions estimated present-day the total C (CO_2 + CO + C) sputtering rate to be 3.4×10^{23} s^{-1} (Leblanc et al., 2019). Dividing the total atmospheric CO_2 3.3×10^{41} molecules by the sputtering rate leads to $\tau_{\mathrm{CO_2,sp}} = 3 \times 10^{10}$ years. Because the dominant escape process of CO_2 (C) on present-day Mars is not sputtering but photodissociation and dissociative recombination (Hu et al., 2015; Lillis et al., 2015), the actual CO_2 lifetime is shorter and estimated to be 1×10^{10} years (Fig. 2).

The lifetime of Ne in Mars' atmosphere is much shorter than C (Jakosky et al., 1994; Hutchins et al., 1997). This is caused by a lower mass of Ne, which leads to a higher scale height above the homopause and a higher yield (Eq. (1)). Recent measurements by MAVEN found that Mars' upper atmosphere is highly variable (e.g., Jakosky et al., 2017; Yoshida et al., 2020). Following Lammer et al. (2020), we assume $T = 200$ K and $\Delta z = 60$–80 km. The temperature was given by averaging the diurnal variations of the exospheric temperature (127 ± 8 to 260 ± 7 K, Stone et al., 2018). The homopause-exobase separation was given from the measurements of the homopause and exobase altitudes (Jakosky et al., 2017). The adopted values result in $R_{\mathrm{diff,Ne/Ar}} = 15$–$35$ (Eq. (2)). Given $(x_{\mathrm{Ne}})_{\mathrm{homo}} = 1$–$6$ ppm (Owen et al., 1977), $(x_{\mathrm{Ar}})_{\mathrm{homo}} = 1.9\%$ (Mahaffy et al., 2013), $U_{\mathrm{es,Ar}}/U_{\mathrm{es,Ne}} = 2$, and $F_{\mathrm{Ar,sp}} = 4.9 \times 10^{22}$ s^{-1} (Leblanc et al., 2019), the sputtering loss rate of Ne is estimated to be $F_{\mathrm{Ne,sp}} = 0.7$–10×10^{20} s^{-1} (Eq. (1)). The estimated lifetime of Ne $\tau_{\mathrm{Ne,sp}}$ is 0.6–1×10^8 years, while heavier noble gases have their lifetime comparable or longer than the age of Mars (Eq. (3) and Fig. 2).

We use the above estimated loss rate for atmospheric Ne to consider the balance between the loss and supply in the following sections. A

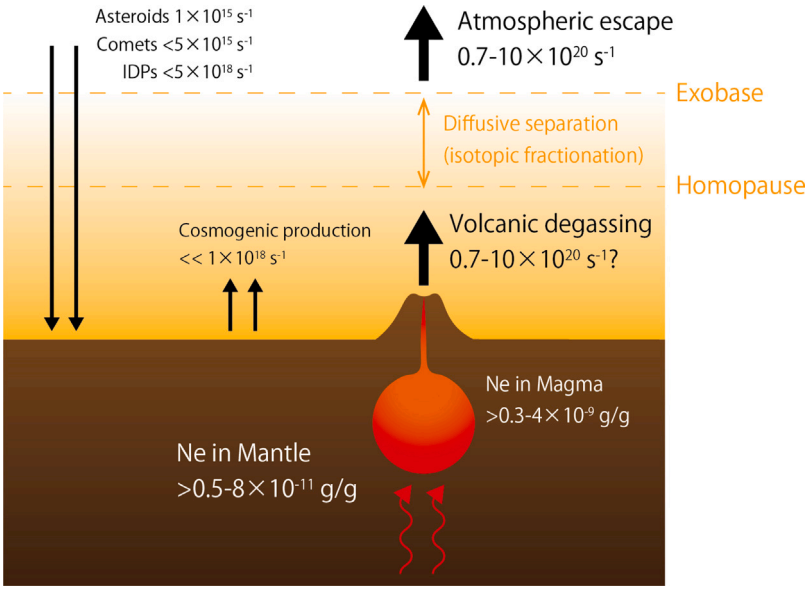

Fig. 1. A schematic overview of loss and supply of Ne in the Martian atmosphere. See text for details.

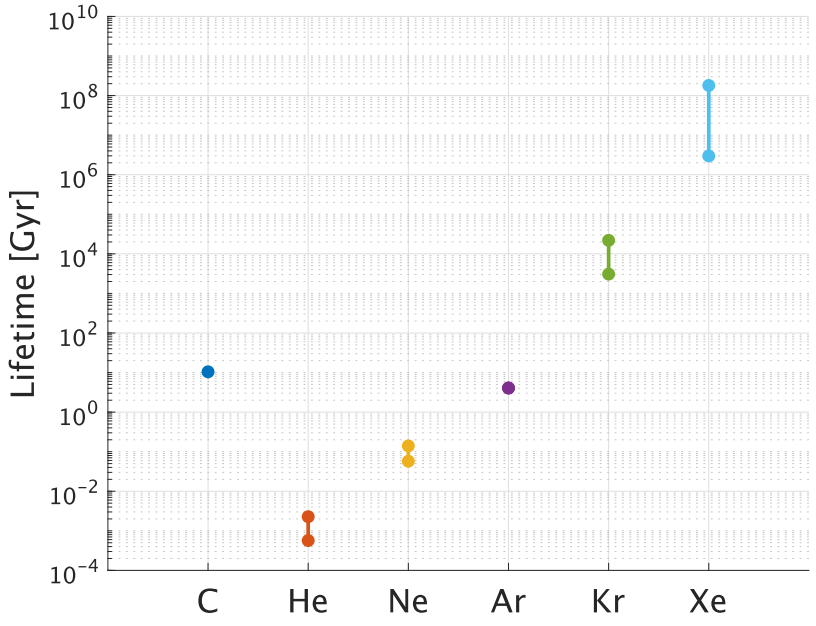

Fig. 2. Lifetime of atmospheric gases against atmospheric escape on present-day Mars. The lifetime of C is estimated with the loss rates via sputtering (see text) and photochemical escape (Hu et al., 2015). The lifetime of He is computed with the estimates of the total loss rate and abundance (Krasnopolsky and Gladstone, 2005). The lifetimes of noble gases other than He are computed from that of Ar with Eq. (3).

background assumption here is that the sputtering rate estimated for current Mars represents the value averaged over a typical Ne lifetime ($\sim 10^8$ years). A process which may influence the validity of this assumption is the variation of CO_2 partial pressure (p_{CO_2}) due to the time-dependent obliquity (Jakosky et al., 1995; Nakamura and Tajika, 2003; Manning et al., 2006). A higher p_{CO_2} reduces Ne mixing ratio in the atmosphere and, consequently, its sputtering rate (Jakosky et al., 1994; Kurokawa et al., 2018). The chaotic nature of obliquity change inhibits its precise determination over more than 10 to 20 Myr (Laskar et al., 2004). Considering that deposits of CO_2 ice that are buried in the south-polar region today (equivalent to p_{CO_2} = 600 Pa, Phillips et al., 2011; Bierson et al., 2016; Jakosky, 2019) could have been in the atmosphere during periods of higher obliquity, the upper limit of p_{CO_2} is twice of the current value. Thus, our estimate for Ne loss rate from Mars in the recent $\sim 10^8$ years may be overestimated by a factor of two in maximum, which is smaller than the uncertainty in Ne loss rate from current Mars and thus acceptable for the accuracy of our estimates given below.

We note that, while we are interested in the loss rates of atmospheric species for recent Mars, these were likely higher for early Mars due to the more active Sun in billions of years ago (e.g., Wood et al., 2002; Ribas et al., 2005; Tu et al., 2015), as recorded in the enrichment of heavy isotopes (e.g., Jakosky et al., 1994, 2017, 2018; Hu et al., 2015; Slipski and Jakosky, 2016; Kurokawa et al., 2018; Lammer et al., 2020). The short lifetime of Ne ($0.6–1 \times 10^8$ years) compared to the timescale of solar evolution ($\sim 10^9$ years) justifies our treatment.

2.3. Supply by asteroids, comets, and interplanetary dust particles

Without continuous supply, atmospheric Ne abundance should decrease in time with the e-folding time identical to the lifetime estimated in Section 2.2. This suggests that Ne had been supplied to the atmosphere until recent ($<\tau_{\mathrm{Ne,sp}}$), or it is being supplied even on present-day Mars. As Ne sputtering loss rate is proportional to atmospheric Ne abundance (Eq. (1)), continuous supply of Ne leads to its balance with sputtering loss (Kurokawa et al., 2018). Assuming the balance between the estimated sputtering rate (Section 2.2) and continuous supply from any source simply leads to the supply rate $F_{\mathrm{Ne,sup}} = F_{\mathrm{Ne,sp}} = 0.7\text{–}10 \times 10^{20}$ s^{-1}. Assuming the supply cessation τ_{cess} ago result in the supply rate $e^{\tau_{\mathrm{cess}}/\tau_{\mathrm{Ne,sp}}}$ times higher in the past, as the current Ne abundance should have evolved from a higher level.

The estimated lifetime $\tau_{\mathrm{Ne,sp}}$ and abundance of atmospheric Ne rule out recent asteroid and comet impacts and interplanetary dust particles (IDPs) accretion as its origins (Fig. 1). Frantseva et al. (2018) estimated mass flux of C-type asteroids and comets onto Mars as 2.5×10^6 kg/yr and 0.13×10^6 kg/yr, respectively. Ne abundance of carbonaceous chondrites is 4×10^{-10} g/g (Marty, 2012). Ne was not detected by Rosetta's in-situ observations of comet 67P/Churyumov-Gerasimenko, which gives an upper limit on Ne abundance as $<3 \times 10^{-8}$ g/g (Rubin et al., 2018). Using these estimates yield Ne supply flux by C-type asteroids and comets as 1×10^{15} s^{-1} and $<5 \times 10^{15}$ s^{-1}, respectively. We note that the contribution of S-type asteroids is negligible, given the lower Ne abundance of ordinary chondrites (Busemann et al., 2000). IDPs' high Ne abundance due to the solar-wind implantation provides higher Ne supply flux, but it is still limited to 5×10^{18} s^{-1} (Flynn, 1997), which is lower than Ne sputtering flux by more than an order of magnitude. We note that the estimate of dust flux onto Mars varies among studies (Flynn, 1997; Borin et al., 2017; Crismani et al., 2017; Frantseva et al., 2018), and here we adopted the highest value. The release of trapped Ne from IDPs requires a heating process after accretion. Thus, the value adopted above, which assumed instantaneous release, is an upper limit of IDPs' contribution.

2.4. Supply of cosmogenic Ne

Degassing of cosmogenic Ne from surface rocks cannot be a major source of atmospheric Ne as well (Fig. 1). Due to the thin atmosphere of Mars, the surface rocks are exposed to galactic cosmic rays, which cause Ne production from spallation of Mg, Si, and Al (Farley et al., 2014). Such cosmogenic contribution has been proposed for Kr and Xe in the Martian atmosphere (Conrad et al., 2016). In the case of Ne, however, the production rate is found to be only $\sim 1 \times 10^{18}$ s^{-1}. Here we adopted a uniform production rate ^{21}Ne 0.02 pmol/g/Ma for the topmost 2 m of the crust (Farley et al., 2014) and ^{20}Ne: ^{21}Ne: ^{22}Ne to be ~1:1:1 (Lal, 1993). Moreover, the measured ^{36}Ar/^{3}He and ^{36}Ar/^{21}Ne at Curiosity's drilling sites are consistent with negligible release of the gases produced in the rock (Farley et al., 2014; Vasconcelos et al., 2016).

2.5. Volcanic degassing and mantle Ne content

Given the limited contribution of the other sources (Sections 2.3 and 2.4), volcanic degassing is the most promising origin of atmospheric Ne (Fig. 1). Here we estimate the lower limit of Ne abundance in the current Martian mantle which can sustain Ne volcanic degassing rate in balance with the sputtering loss to space.

Though the major volcanic activity is limited to the late Noachian and Hesperian, high-resolution crater-based studies have identified recent ($\sim 10^{7\text{–}8}$ years) caldera floors and lava flows in the Tharsis region (Hauber et al., 2011; Robbins et al., 2011; Grott et al., 2013). After the submission of this study, evidence of very recent volcanic activity as young as 5×10^4 years in Elysium Planitia was reported (Horvath et al., 2021). These studies imply that a certain level of volcanic activity persisted up to present day. The magma eruption rate of those recent activity has not been estimated, and here we adopt that for the late Amazonian as an upper limit. Dividing the maximum estimate for total (extrusive and intrusive) magma volume 2.7×10^7 km^3 (Greeley and Schneid, 1991) by the duration of the late Amazonian 0.3–0.6 Gyrs (Hartmann and Neukum, 2001) leads to 0.045–0.09 km^3/yr, and thus the upper limit is 0.09 km^3/yr. Here we assumed the highest estimate of intrusive-to-extrusive eruption ratio, 12:1 (Greeley and Schneid, 1991). Adopting a typical magma density 3.3 g/cm^3 and complete degassing even from intrusive magma, Ne abundance in the source magma (the magma chamber in Fig. 1) to balance volcanic supply of Ne with the sputtering loss is estimated to be $>0.3\text{–}4 \times 10^{-9}$ g/g, where the range comes from the model uncertainty in Ne loss rate (Section 2.2).

The source magma is produced by partial melting of mantle upwelling. An upwelling mantle plume experiences partial melting (Li and Kiefer, 2007), forming many small melt particles within it. Each small melt particle is equilibrated with the surrounding residual rocks. Owing to its high incompatibility, Ne is almost fully partitioned into the melt (Heber et al., 2007; Moreira and Kurz, 2013). Melt is channeled and coalesces to form a dike, which sources magma to a shallow-level magma chamber or directly erupts into the surface (O'Neill et al., 2007). The melt fraction of the source mantle is estimated to be 0.02–0.1 from the analysis of rare earth elements in Martian basaltic meteorites (Norman, 1999; Borg and Draper, 2003). Thus, multiplying the above estimated Ne abundance in the magma by the lower limit of the melt fraction 0.02 ends up with Ne abundance of the current mantle $x^{\mathrm{present}}_{\mathrm{Ne,mantle}}$ $>0.5\text{–}8 \times 10^{-11}$ g/g (Figs. 1 and 3).

3. Ne content in the magma ocean stage

The Martian mantle is rich in Ne. In Section 2.5, we estimated the abundance $x^{\mathrm{present}}_{\mathrm{Ne,mantle}}$ to be $>0.5\text{–}8 \times 10^{-11}$ g/g. The total Ne mass in the mantle $M^{\mathrm{present}}_{\mathrm{Ne,mantle}}$ is $>3\text{–}40 \times 10^{12}$ kg (assuming the mantle mass fraction 0.76, Rivoldini et al., 2011). As the total Ne mass in the atmosphere is $1\text{–}6 \times 10^{10}$ kg, this estimate means that the mantle is possibly the largest reservoir of Ne on Mars. For comparison, Earth's largest reservoir of Ne is its atmosphere, and Ne abundance in Earth's present-day bulk mantle has been estimated to be 1×10^{-12} g/g from calibration to ^{40}Ar (Marty, 2012). Thus, Ne abundance in the Martian mantle is higher than in Earth's by more than a factor of 5–80. We note that here we compared their present-day abundances, and the relation may not be applicable to their original values (at the time when their magma oceans solidified) because the mantle Ne abundances would have declined with time due to secular degassing (see also Section 5.4).

The high Ne abundance suggests that the Martian mantle is rich in other volatile elements as well (Section 4) and that secular degassing from such a volatile-rich mantle could have been an important driver of Mars' climate. Moreover, as we explain below, the smaller size of Mars relative to Earth requires an even larger amount of total Ne in the magma ocean stage to put Ne into the mantle.

The abundant Ne in the Martian mantle likely have its origin in the planet formation stage. Plate tectonics and crustal recycling have not been operating on Mars at least for the past 4 billion years (e.g., Grott et al., 2013). Subduction-driven Ne recycling is inefficient even on tectonically-active Earth (Bekaert et al., 2020). The solar-like ^{20}Ne/^{22}Ne ratio of the deep mantle endmember (13.23 ± 0.22, Williams and Mukhopadhyay, 2019) is distinct from that in Earth's atmosphere (9.8) and suggests that Earth's mantle Ne originated at least partially from captured proto-solar nebula gas (Yokochi and Marty, 2004).

Incorporating the large amount of Ne into the mantle requires an even larger amount of total Ne during the formation stage. This is because of Ne's low solubility in silicate melt and incompatibility. Here we consider Ne partitioning between the atmosphere, magma ocean, and solidified mantle in the magma ocean stage. The partial pressure

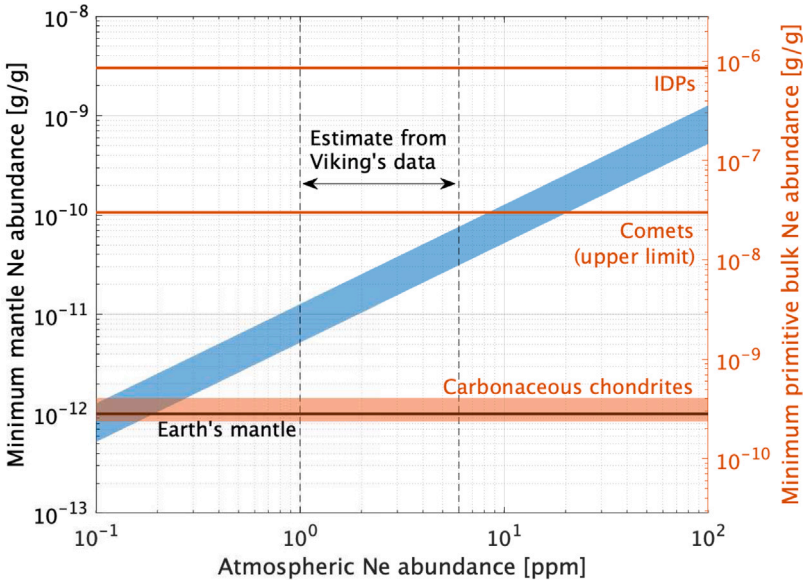

Fig. 3. Minimum estimates for mantle (left axis, Section 2) and primitive bulk (right axis, Section 3) Ne abundances as a function of that of atmospheric Ne (blue area). The balance between the atmospheric loss and volcanic supply is assumed. The range of blue area comes from the uncertainty in the elemental fractionation factor of sputtering. Dashed lines denote the range of atmospheric Ne abundance estimated from Viking data (Owen et al., 1977). Earth's bulk mantle Ne abundance (Marty, 2012) is shown for comparison to the Martian mantle value (left axis). Orange lines are Ne abundances in possible sources to compare with the Martian primitive bulk value (right axis). Carbonaceous chondrites: Marty (2012). Comets: Rubin et al. (2018). IDPs: Flynn (1997). (For interpretation of the references to color in this figure legend, the reader is referred to the web version of this article.)

of Ne in the atmosphere in equilibrium with the magma ocean $P_{\rm Ne}$ is given by,

$$P_{\rm Ne} = \frac{x_{\rm Ne,mo}}{S_{\rm Ne}}, \tag{5}$$

where $x_{\rm Ne,mo}$ is Ne mass fraction in the magma ocean and $S_{\rm Ne}$ is the solubility. The total Ne mass in the atmosphere $M_{\rm Ne,atm}$ is given by,

$$M_{\rm Ne,atm} = \frac{m_{\rm Ne}}{\overline{m}} \frac{A p_{\rm Ne}}{g}, \tag{6}$$

where $\overline{m}$ is the mean molecular mass of atmospheric gases (here we adopt $\overline{m} = 44$ amu assuming the dominant gas is CO_2) and A is the surface area of the planet. Given Eq. (5), (6), and $M_{\rm Ne,mo} = x_{\rm Ne,mo} \cdot M_{\rm mo}$ (where $M_{\rm mo}$ is the mass of magma ocean), the atmospheric and magma ocean Ne mass ratio is given by,

$$\frac{M_{\rm Ne,atm}}{M_{\rm Ne,mo}} = \frac{m_{\rm Ne} A}{\overline{m} g S_{\rm Ne} M_{\rm mo}}. \tag{7}$$

Assuming a pyrolite magma composition (McDonough and Sun, 1995) and the temperature of 1,700 K in a semi-empirical solubility model of Iacono-Marziano et al. (2010), the solubility $S_{\rm Ne}$ is estimated to be 1.6 ppm/MPa, which leads to $M_{\rm Ne,atm}/M_{\rm Ne,mo} > 20$, where the minimum value is given by assuming a fully molten magma ocean ($M_{\rm mo} = M_{\rm mantle}$, where $M_{\rm mantle}$ is the mass of the mantle).

Moreover, the mineral-melt partitioning coefficient of Ne is extremely low ($\sim 10^{-4}$, Heber et al., 2007), which means that magma ocean solidification induces significant degassing. Thus, the mass of Ne trapped in the solidified mantle would be dominated by Ne in interstitial melt rather than in crystallized minerals. Given the trapped melt fraction $F_{\rm tl}$, here defined as the mass fraction of trapped interstitial melt relative to the total solidified mass (trapped and then solidified melt plus crystallized minerals) at the solidification front, Ne mass in the solidified mantle $M_{\rm Ne,sm}$ upon magma ocean solidification is given by,

$$d M_{\rm Ne,sm} = F_{\rm tl} \cdot x_{\rm Ne,mo} \cdot d M_{\rm sm}. \tag{8}$$

We note that the subscript sm is used for the solidified mantle under the magma ocean, whereas the subscript mantle is for the mantle after complete solidification. Assuming $F_{\rm tl}$ to be constant through the bottom-up solidification, Eq. (8) can be integrated analytically. The mass of Ne in the mantle after complete mantle solidification is given by (see Appendix for derivation),

$$M_{\rm Ne,mantle} = \left[1 - \left(\frac{1}{1 + \overline{m} g S_{\rm Ne} M_{\rm mantle}/m_{\rm Ne} A}\right)^{F_{\rm tl}}\right] M_{\rm Ne,tot}, \tag{9}$$

where $M_{\rm Ne,tot}$ is the total mass of Ne in the system. In the low solubility limit ($\overline{m} g S_{\rm Ne} M_{\rm mantle}/m_{\rm Ne} A \ll 1$, which is satisfied for Ne), Eq. (9) is approximated by,

$$M_{\rm Ne,mantle} \simeq F_{\rm tl} \frac{\overline{m} g S_{\rm Ne} M_{\rm mantle}}{m_{\rm Ne} A} M_{\rm Ne,tot}. \tag{10}$$

The trapped melt fraction is typically assumed to be ~1%, but it would be dependent on the evolutionary properties of magma ocean (e.g., the cooling timescale, Hier-Majumder and Hirschmann, 2017). Assuming the maximum estimate $F_{\rm tl} = 0.3$, which corresponds to the value for the rheological transition, we obtain $M_{\rm Ne,tot} > 3 \times 10^2\ M_{\rm Ne,mantle}$ for Mars. Thus, assuming that $M_{\rm Ne,mantle} = M^{\rm present}_{\rm Ne,mantle}$, >300 times more Ne is required to put the estimated Ne abundance into the Martian mantle (Fig. 3). We note that such preferential partitioning into the atmosphere in the magma ocean stage has been modeled also for C (Elkins-Tanton, 2008; Hier-Majumder and Hirschmann, 2017). The excess amount of Ne in the atmosphere would have been lost after the magma ocean solidification by atmospheric escape processes such as impact erosion, hydrodynamic escape, and sputtering.

Secular degassing after the magma ocean solidification requires an even higher primitive Ne content ($M_{\rm Ne,mantle} > M^{\rm present}_{\rm Ne,mantle}$). Integrating the estimated volcanic degassing rate (Section 2.5) of Ne on current Mars over 4.5 Gyrs leads to ≃10% depletion of the estimated mantle Ne content. While the degree of cumulative volcanic degassing cannot be directly constrained and is dependent on models (Grott et al., 2013), higher volcanic activity of early Mars (Greeley and Schneid, 1991) would cause more depletion. Thus, the estimated primitive Ne content ($M_{\rm Ne,tot} > 3 \times 10^2\ M_{\rm Ne,mantle}$) is the lower limit.

Another useful measure of the required Ne mass is the partial pressure. Combining Eq. (5) and (10), we obtain,

$$p_{\rm Ne} \simeq \frac{x_{\rm Ne,mantle}}{F_{\rm tl} S_{\rm Ne}}. \tag{11}$$

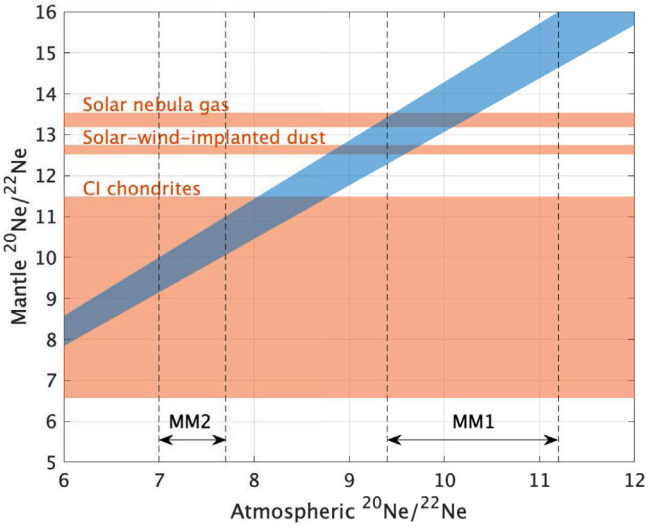

Fig. 4. $^{20}Ne/^{22}Ne$ ratios in the Martian atmosphere and mantle. The blue area denotes the steady-state relation where the atmospheric loss and supply are balanced (Eq. (4)). Its range comes from the uncertainty in the isotopic fractionation factor of sputtering. The ranges of atmospheric values suggested from trapped gas in Martian meteorites are indicated by vertical lines. MM1: Wiens et al. (1986), Swindle et al. (1986). MM2: Park and Nagao (2006), Park et al. (2017). The isotope ratios of possible sources are shown to compare with the mantle values (orange areas). Solar nebula gas: Heber et al. (2012). Solar-wind-implanted dust: Moreira and Charnoz (2016), Péron et al. (2017). CI chondrites: Mazor et al. (1970). (For interpretation of the references to color in this figure legend, the reader is referred to the web version of this article.)

Substituting $F_{\rm tl} < 0.3$ and $x_{\rm Ne,mantle} > x^{\rm present}_{\rm Ne,mantle}$ for Eq. (11) gives the required Ne partial pressure of the Martian primitive atmosphere overlying the magma ocean to be > 10 Pa. This required Ne partial pressure corresponds to 300 times the current mantle Ne content derived above. The pressure is compared with that of the captured solar nebula gas in Section 4.

Eq. (10) exhibits the dependence on the planet size $M_{\rm Ne,tot}/M_{\rm Ne,mantle} \propto M_{\rm p}^{-\frac{2}{3}}\overline{\rho}^{-\frac{4}{3}}$, where $M_{\rm p}$ and $\overline{\rho}$ are the mass and the bulk density of the planet, respectively. The right-hand side factor is ~7 times larger for Mars than for Earth, due to the smaller gravity and the higher surface area to mass ratio. This means that putting the same amount of Ne into the Martian mantle requires a total amount of Ne 7 times larger than that for Earth.

4. Origin of abundant Martian Ne

Here we combine the isotopic constraint on Ne source (Section 2.1) and the estimates of the required Ne content and atmospheric partial pressure in the magma ocean stage (Section 3) to discuss the possible origins of abundant Martian Ne.

Atmospheric $^{20}Ne/^{22}Ne$ ratios informed from Martian meteorites (Section 2.1) are consistent with either the solar nebula gas, the solar-wind implanted dust, or the chondritic origin, yet the uncertainty in the true atmospheric value prevents the conclusive determination of the origin(s) (Fig. 4). If the atmospheric $^{20}Ne/^{22}Ne$ ratio is ~10 (MM1 in Fig. 4), the estimated mantle $^{20}Ne/^{22}Ne$ ratio suggests the captured solar nebula or the solar-wind-implanted dust origin. If the atmospheric $^{20}Ne/^{22}Ne$ ratio is ~7 (MM2 in Fig. 4), The estimated mantle $^{20}Ne/^{22}Ne$ ratio suggests the chondritic origin.

Prior to future precise determination, below we discuss the implications for the abundance of volatile elements in Mars and for accretion history of Mars from the three possible Ne origins.

4.1. Capture of solar nebula gas

A planet formed in a protoplanetary disk captures disk gas as the atmosphere (hereafter called the primordial atmosphere) by its gravity (e.g., Hayashi et al., 1979; Sasaki, 1999). Its $^{20}Ne/^{22}Ne$ ratio should be identical to the solar value (13.36 ± 0.16, Fig. 4). The primordial atmospheres are not present on the terrestrial planets in our Solar system. However, the $^{20}Ne/^{22}Ne$ ratio of Earth's deep mantle Ne is consistent with the solar nebula origin (Yokochi and Marty, 2004; Williams and Mukhopadhyay, 2019). Earth's water as well as hydrogen (H) in the core has been proposed to originate at least partially from H in the primordial atmosphere (Genda and Ikoma, 2008; Hallis et al., 2015; Sharp, 2017; Wu et al., 2018; Olson and Sharp, 2018, 2019; Saito and Kuramoto, 2020). A low deuterium to hydrogen (D/H) ratio signature of a Martian meteorite has been also attributed to the nebula-gas origin (Hallis et al., 2012, 2015), though a higher, chondrite-like D/H ratio is considered as a typical mantle value (Usui et al., 2012). A solar-like Xe isotopic composition found in Chassigny, which is interpreted to originate from the Martian interior (Ott, 1988), may also support capture of the solar nebula gas. The elemental abundance pattern of Venus' atmospheric noble gases suggests the remnant of the primordial component (Pepin, 1991; Genda and Abe, 2005). The primordial atmospheres are ubiquitous in extrasolar planetary systems, known as super Earths and mini-Neptunes (e.g., Rogers, 2015).

While forming a dense primordial atmosphere is relatively easy for an Earth-sized planet, it is possible for a Mars-sized planet only under some specific conditions as we show below. This is because the amount of the captured primordial atmosphere highly depends on the planetary mass (Sasaki and Nakazawa, 1990; Ikoma and Genda, 2006). Therefore, the solar-nebula-gas originated Ne in the Martian mantle can, if proved, serve important constraints on its formation history.

Assuming a spherically-symmetric, radiative-equilibrium structure (Sasaki and Nakazawa, 1990), the surface pressure of the primordial atmosphere surrounding a planet embedded in a protoplanetary disk is approximated by,

$$p_{\rm s} \simeq \frac{\pi^2\sigma}{36}\left(\frac{G\mu m_{\rm H}}{k_{\rm B}}\right)^4 \overline{\rho} M_{\rm p}^2 \kappa^{-1} \tau_{\rm acc}, \tag{12}$$

where $k_{\rm B}$ is the Boltzmann constant, σ is the Stefan–Boltzmann constant, G is the gravitational constant, $m_{\rm H}$ is the mass of a H atom, μ is the mean molecular weight, κ is the opacity, and $\tau_{\rm acc}$ is the accretion time scale which gives the luminosity $L = GM_{\rm p}^2/R_{\rm p}\tau_{\rm acc}$. We note that Eq. (12) has planetary-mass dependence different from that in Equation 15 of Sasaki and Nakazawa (1990) (the power-law index 2 vs. 3), the latter of which seems to be a typo. Substituting Mars mass and density into Eq. (12) leads to,

$$p_{\rm s} \simeq 1\times10^3 \left(\frac{\mu}{2.35}\right)^4 \left(\frac{\kappa}{0.1\ {\rm m^2/kg}}\right)^{-1} \left(\frac{\tau_{\rm acc}}{1\ {\rm Myr}}\right) {\rm Pa}, \tag{13}$$

where we adopted the mean molecular weight of solar nebula gas, an interstellar-medium-like opacity (e.g., Stevenson, 1982), and an estimated growth timescale for Mars (1–3 Myrs, Dauphas and Pourmand, 2011) as the scaling factors. Substituting the molar fraction of ^{20}Ne in the solar nebula $f_{\rm Ne,SN} = 1.8\times10^{-4}$ (Wieler, 2002; Yokochi and Marty, 2004) into Eq. (13), we obtain the Ne partial pressure as,

$$p_{\rm Ne} \simeq 2\times10^{-1} \left(\frac{f_{\rm Ne}}{f_{\rm Ne,SN}}\right) \left(\frac{\mu}{2.35}\right)^4 \left(\frac{\kappa}{0.1\ {\rm m^2/kg}}\right)^{-1} \left(\frac{\tau_{\rm acc}}{1\ {\rm Myr}}\right) {\rm Pa}. \tag{14}$$

Eq. (14) shows that Ne partial pressure of the Martian primordial atmosphere under a typical condition is two orders of magnitude lower than the value required to put the estimated Ne into the mantle (~ 10 Pa, Section 3).

What are the formation scenarios of Mars which enable the accretion of a dense primordial atmosphere? A possibility is the completion of accretion prior to the dissipation of the solar nebula, which lowers the accretion luminosity (long $\tau_{\rm acc}$ in Eq. (14) at the late stage).

This scenario may be consistent with Mars accretion time estimated from hafnium–tungsten–thorium (Hf–W–Th) chronology (Dauphas and Pourmand, 2011) being earlier than the dissipation time of the solar nebula suggested from meteorite paleomagnetism (Weiss et al., 2021). The opacity κ, which is mainly determined by the dust abundance, can be also lowered, if the surrounding solar nebula at the time of gas dissipation was depleted in small dust. Both of the two possibilities point to a low surface density of solid materials in Mars forming region, which provides constraints on dust coagulation and transport processes in the solar nebula.

Another possibility to increase Ne partial pressure is mixing of a high-molecular-weight component degassed from Mars building blocks. For instance, mixing degassed CO_2 (other components are ignored for simplification) and the captured solar nebula gas with 1:1 ratio leads to $f_{Ne}/f_{Ne,SN} = 0.5$ and $\mu/2.35 \sim 20$, and thus $p_{Ne} \sim 1 \times 10^4$ Pa (Eq. (13)). Though Saito and Kuramoto (2018, 2020) concluded that the two components are likely stratified rathen than mixed, eddy diffusion or mechanical mixing either due to impacts or nebula gas flow (Ormel et al., 2015; Kurokawa and Tanigawa, 2018; Kuwahara et al., 2019; Mai et al., 2020) may induce the mixing.

If the mantle Ne resulted from the nebula gas capture, the mantle would acquire other volatile elements from the nebula gas depending on their solubility into the magma ocean, partitioning coefficients between minerals and silicate melt, and those between core-forming metals and silicate melt. The solubilities of major volatile elements H (which forms water), nitrogen (N), and sulfur (e.g., Hirschmann, 2016) are higher than that of Ne (Iacono-Marziano et al., 2010). This means that these elements can be trapped from solar nebula gas more efficiently than Ne.

4.2. Solar-wind-implanted dust

Exposure of small dust grains to the solar wind implants its ions to their surfaces. A combination of the solar-wind implantation and erosion of the outer layers of the grains, where ^{20}Ne enriches, results in the ^{20}Ne/^{22}Ne ratio slightly lower than the solar value (12.52–12.75, Fig. 4). The solar-wind-implanted dust has been proposed to the origin of Earth's mantle Ne alternative to the nebula gas (Trieloff et al., 2000; Moreira and Charnoz, 2016; Jaupart et al., 2017; Péron et al., 2017; Vogt et al., 2019). We note that both solar-wind-implanted dust and IDPs are the same materials, but the former and latter denote those in the planet formation stage and in the current Solar System, respectively, in our definition following the terminology in the literature.

The solar-wind implanted dust grains could be rich in Ne, as known for IDPs (Flynn, 1997). Assuming Ne abundance of IDPs ($\sim 9 \times 10^{-7}$ g/g), the estimated primordial bulk abundance of Ne can be supplied if Mars building blocks are consist of ~0.1–1 wt% irradiated materials (Fig. 3). The actual Ne abundances of these grains depend on their grain sizes, distances from the Sun, and exposure time (Moreira and Charnoz, 2016).

If Martian Ne originated from the solar-wind-implanted dust, it provides constraints on dust grain sizes and turbulent strengths in the solar nebula when Mars formed, both of which are important parameters for the planet formation (e.g., Ormel and Klahr, 2010; Lambrechts and Johansen, 2014; Guillot et al., 2014; Kuwahara and Kurokawa, 2020a,b). Mars likely formed before the dissipation of the solar nebula (Dauphas and Pourmand, 2011; Kobayashi and Dauphas, 2013). Thus, Mars forming region was protected from the solar wind irradiation by the solar nebula. The exposure of Martian building materials to the solar wind requires dust grains being small enough and turbulence in the solar nebula to be strong enough in order to dredge up them from the midplane to higher altitudes of the solar nebula disk (Moreira and Charnoz, 2016). Grain sizes and turbulent strength in protoplanetary disks have been studied actively with telescopic observations (Kataoka et al., 2016; Dullemond et al., 2018; Okuzumi and Tazaki, 2019; Ohashi and Kataoka, 2019; Rosotti et al., 2020; Ueda et al., 2020; Doi and Kataoka, 2021), but these studies focus on outer regions of protoplanetary disks as the spatial resolution of observations is typically limited to several tens to hundreds au. Thus, the presence of the solar-wind Ne component in the Martian mantle is, if proved, an important clue to understand the property of inner, terrestrial planet forming regions of protoplanetary disks (~ 1 au).

Alternatively, formation of Mars after the nebula dissipation may be responsible for the accretion of the solar-wind-implanted dust. Marchi et al. (2020) proposed that impact generation of mantle domains with variably fractionated Hf/W ratios and diverse ^{182}W can relax the constraint on the formation timescale (Dauphas and Pourmand, 2011).

Solar wind implantation is in principle applicable to any types of materials. Therefore, the amounts of other volatile elements supplied to accreting Mars are not directly constrained in this scenario, though the solar-wind-implanted bodies are in general rich in volatile elements (see Section 4.3). Additionally, volatile elements other than Ne (e.g., H) can be implanted to Mars building blocks and supplied to Mars as well.

4.3. Chondrites and comets

Because chondrites are thought to be fundamental building blocks of terrestrial planets, their contribution as Ne source is naturally expected. Carbonaceous chondrites show ^{20}Ne/^{22}Ne = 9.03 ± 2.46 (Fig. 4) as a non-cosmogenic endmember. The origin of this endmember has been proposed to be a mixture of the presolar component and the other (so called Q-gas or the solar wind) component (Moreira and Charnoz, 2016, and references therein). Ordinary and enstatite chondrites show broadly similar ^{20}Ne/^{22}Ne ratios, but the contribution of the solar component seems to be higher (Moreira and Charnoz, 2016).

However, even considering the most volatile-rich, carbonaceous chondrites does not provide enough Ne to explain the estimated Martian mantle Ne content (Fig. 3). Therefore, if the Martian mantle is proved to have a chondritic ^{20}Ne/^{22}Ne ratio, it suggests unknown Martian building blocks that are rich in Ne with a chondritic isotope composition. This is also related to the elemental composition of bulk Mars — for instance, Ne in carbonaceous chondrites is trapped in carbon phases (e.g., Busemann et al., 2000) and thus a hypothetical Ne-rich materials may be rich in C as well.

Comets are potential candidates of such Ne-rich bodies which might constitute some fraction of Martian building blocks. In situ measurements of gases in the coma of comet 67P/Churyumov-Gerasimenko did not detect Ne (Rubin et al., 2018), and thus only the upper limit on Ne abundance was provided (Fig. 3). Ne trapped in ice is thought to have a solar-like isotopic composition (Dauphas, 2003). In contrast, refractory grains returned by the Stardust mission to comet Wild 2 show rather chondritic Ne isotopic compositions with their abundances comparable to IDPs (Marty et al., 2008; Palma et al., 2019). The determination of the bulk abundance and isotopic composition of Ne in comets would thus be important to understand the origin of Martian Ne.

In both cases, Ne is relatively depleted in chondrites and possibly in comets compared to the solar abundance (e.g., Dauphas, 2003; Marty, 2012). Thus, the Ne-rich mantle (Section 2.5) suggests enrichment of other volatile elements as well.

5. Discussion

5.1. Measurements of atmospheric ne by future missions

Given its importance for constraining the abundance and origin of Ne in the mantle (Section 4), more precise determination of the elemental and isotopic abundances of Ne in the Martian atmosphere is desired. Though indirect determination using trapped gas in Martian meteorites has provided useful estimates (Section 2.1), in situ measurements would, if performed, provide undoubted constraints. Here we discuss the feasibility of in situ measurements by a future exploration mission. As mentioned in Section 2.1, only the abundance of ^{22}Ne

has been determined for Ne with in situ analysis. The most abundant isotope ^{20}Ne has not been measured so far due to the interference of $^{40}Ar^{++}$ to $^{20}Ne^{+}$ in mass spectrometry. The abundance of ^{40}Ar is much higher than that of ^{20}Ne in the atmosphere (2.5 ppm for ^{20}Ne and 2% for ^{40}Ar, respectively; Owen et al., 1977; Franz et al., 2017). Therefore, Ar must be removed for the Ne isotope measurements. Although Ar is separated cryogenically by using liquid nitrogen and/or a cryo-trap in laboratory experiments, it is difficult to apply this method to space missions. As a preferable way to separate Ne from Ar, Miura et al. (2020) proposed a method using a permeable membrane. They experimentally investigated permeation of Ne and Ar through polyimide and Viton sheets under the terrestrial atmosphere, where polyimide sheets more efficiently separated Ne from Ar.

Determining whether the Martian mantle Ne is solar-like (solar nebula or implanted solar wind, $^{20}Ne/^{22}Ne \sim 13$) or chondritic ($^{20}Ne/^{22}Ne \sim 7$–11) requires the measurements of the atmospheric Ne isotopic ratio with <10% uncertainty (Fig. 4). On the basis of the experimental data, a polyimide sheet with a thickness of ~75 μm and an area of $\gtrsim$50 cm^2 has been suggested as a possible membrane for the Ne-Ar separation under the Martian atmospheric condition (Miura et al., 2020). Within a reasonable time (e.g., within an hour), a detectable amount of Ne does not permeate through a polyimide sheet much thicker than 75 μm, on the other hand, a significant amount Ar as well as Ne permeates through the sheet thinner than 75 μm. The necessary size of the membrane depends on the sensitivity of the mass spectrometer. The amount of permeating ^{20}Ne through the polyimide sheet with 75 μm in thickness and 50 cm^2 in area during 60 min has been estimated as $\sim 1 \times 10^{-9}$ cm^3 STP, which corresponds to an ion counts of 1.3×10^5 cps if Ne is expanded to a volume of 1000 cc and a mass spectrometer with the sensitivity of 5×10^{-3} (counts/sec)/(particle/cc) is used. For comparison, sensitivities of $\sim 5 \times 10^{-3}$ and $\sim 1 \times 10^{-2}$ (counts/sec)/(particle/cc) have been reported for the quadrupole mass spectrometer on the Curiosity rover (Mahaffy et al., 2012) and the Reflectron-type Time-Of-Flight mass spectrometer (RTOF) on the Rosetta Orbiter Spectrometer for Ion and Neutral Analysis (ROSINA) (Balsiger et al., 2007), respectively. Sensitivities of 2×10^{-3} for ^{4}He and 3×10^{-2} for ^{40}Ar at the emission current of 250 μm and calibration procedures about Neutral Gas and Ion Mass Spectrometer (NGIMS) on MAVEN have been reported (Mahaffy et al., 2015). The amount of ^{22}Ne is likely ~1/10 of ^{20}Ne (Section 2.1), so that the ion count of ^{22}Ne is estimated to be $\sim 1 \times 10^4$ cps. The uncertainties for $^{20}Ne/^{22}Ne$ ratios are arisen from a statistical error and corrections for mass discrimination, blank, and doubly charged ions ($^{40}Ar^{++}$ and CO_2^{++}). The statistical error for the isotope ratio is ~1% in the case of the above amount of ^{20}Ne permeated. The contributions of blank ^{20}Ne, $^{40}Ar^{++}$, and CO_2^{++} are considered to be about 10%, 10%, and a few % of permeating ^{20}Ne (for ^{20}Ne and $^{40}Ar^{++}$) or ^{22}Ne (for CO_2^{++}), respectively, when the amounts of blank are assumed to be similar to those in the laboratory experiment performed by Miura et al. (2020). Because the source of the blank ^{20}Ne and the contribution of $^{40}Ar^{++}$ are from the terrestrial atmosphere dissolved into a sealing material made from Viton, these values are likely upper limits and can be improved by revising the sealing material and/or considering the pressure of the Martian atmosphere being two orders of magnitude lower than that of the terrestrial atmosphere. Since CO_2 is mostly removed using a getter, the main contribution is of the background CO_2 from the ion source of the mass spectrometer. Assessing these error factors, where 50% uncertainty to each correction is assumed, the $^{20}Ne/^{22}Ne$ ratio is expected to be obtained with <10% uncertainty. Therefore, this methodology for in situ mass spectrometry utilizing a permeable membrane can identify either solar-nebular- or implanted-solar-wind-like Ne or chondritic Ne as the source of Martian atmospheric Ne (Fig. 4).

Distinguishing captured-solar-nebula ($^{20}Ne/^{22}Ne = 13.36 \pm 0.16$) and implanted-solar-wind ($^{20}Ne/^{22}Ne \sim = 12.52$–12.7) components is more challenging, and requires the determination of the atmospheric Ne isotopic ratio with <1% uncertainty (Fig. 4). This might be possible by adopting a mass spectrometer with high sensitivity and/or high resolution, developing a method for more efficient Ne-Ar separation, tuning of ion source parameters to lower production rates of the doubly charged ions (e.g., a lower electron energy reduces ++/+ ratios; Meshik et al., 2012; Miura et al., 2020), utilizing a wider membrane area and/or better reduction of blank. It is also crucial to improve the model for Ne escape to reduce the uncertainty in isotopic fractionation factor, which directly influences the uncertainty in converting the atmospheric to mantle Ne isotopic ratios (Eq. (4)).

We utilized the absolute abundance of ^{20}Ne in the Martian atmosphere estimated from ^{22}Ne abundance measured with Viking (Fig. 3), but direct determination of ^{20}Ne abundance is desired. For this purpose, in situ calibration of the mass spectrometer during the mission and accurate determination of the permeability and diffusion coefficient using a flight-model membrane in a laboratory are essential. Based on their experience at the laboratory, Blanchard et al. (1986) reported that operation of the quadrupole mass spectrometer system with tungsten filaments at constant temperature has yielded more stable operation with weekly sensitivity changes being less than 10%. Even for a space mission, it is recommended to carry a calibration gas for Ne to obtain a reliable ^{20}Ne abundance. The calibration-gas-system consists of a gas reservoir and some micro valves as utilized in the Curiosity and MAVEN missions (Mahaffy et al., 2015). In addition, the linearity of signals against gas amounts in the mass spectrometer must be examined carefully, although noble gases generally show a liner trend over several orders and the amount of calibration gas should be controlled to come to similar amounts between calibration and sample gases. As a result, we expect that the abundance of Ne will be determined within the uncertainty of a factor of two, which will improve the estimate for the mantle Ne abundance and constrain its source (Fig. 3).

Mars Sample Return (MSR, Beaty et al., 2019) is another potential opportunity to measure the elemental and isotopic abundance of Ne on Mars. Rock samples potentially contain atmospheric and/or mantle-derived volatiles in trapped gas as we know it from Martian meteorites. However, both Martian meteorites and surface rocks analyzed in situ by Curiosity showed the dominance of cosmogenic Ne (Farley et al., 2014; Smith et al., 2020), which inhibited the determination of atmospheric or mantle-derived components. The possibility to recover Mars' atmospheric and/or mantle Ne endmembers would be dependent on the properties of returned rock samples such as the intrinsic to cosmogenic gas ratio and the total amount of trapped gas. Sample return of atmospheric gas itself would be, If performed, a more promising opportunity to measure Ne abundance in the Martian atmosphere.

5.2. Constraints from other volatile elements

$^{20}Ne/^{22}Ne$ ratio may not solely provide conclusive determination of the origin of abundant mantle Ne especially if Ne was sourced from multiple materials. Thus, combining multiple volatile elements is useful for constrain the origin of abundant mantle Ne.

Isotopic compositions of H and N in the Martian mantle are informed to be broadly chondritic (Usui et al., 2012; Mathew and Marti, 2001). This would be naturally reconciled if the mantle Ne also originated from chondritic materials. The chondritic origin for H and N in the Martian mantle would limit the contribution of comets, whose D/H and $^{15}N/^{14}N$ ratios are distinctly higher than chondrites (Füri and Marty, 2015), though the determination of bulk Ne abundance in comets is needed for further quantification. In contrast, solar nebula gas has D/H and $^{15}N/^{14}N$ ratios lower than chondrites (Füri and Marty, 2015). This may limit the contribution of solar nebula gas on Martian volatiles, though mixing with cometary volatiles and/or isotopic fractionation via atmospheric escape (e.g., Genda and Ikoma, 2008; Lammer et al., 2020) can elevate these ratios.

Hutchins et al. (1997) estimated $^{20}Ne/^{36}Ar$ degassing ratio to be 10–26 by modeling the evolution of Ne and Ar isotopic ratios in the

Martian atmosphere. If the ratio reflects the incorporation during the magma ocean stage, multiplying their solubilities (1.6 ppm/MPa vs. 0.2 ppm/MPa from the model of Iacono-Marziano et al., 2010) leads to the original (source) ratio of $^{20}Ne/^{36}Ar \simeq 1.3–3.3$. This ratio is lower than that of solar gas (~10, Lodders, 2003), and thus suggests the contribution of chondritic, cometary, or IDP-like materials. Though the estimated degassing ratio may not be applicable if we consider Ar supply by late accretion (Kurokawa et al., 2018; Sakuraba et al., 2019), combining multiple noble gases is potentially useful for constraining the origin of Ne.

5.3. Implications for the surface environment of early mars

We showed that a large amount of Ne in the atmosphere might exist on Mars when it formed. The lower limit of Ne partial pressure is ≃10 Pa, which is higher than the current value ($0.6–4 \times 10^{-3}$ Pa) by about four orders of magnitude. This excess amount of atmospheric Ne can be easily removed by atmospheric escape processes such as hydrodynamic escape (Pepin, 1991), impact erosion (Melosh and Vickery, 1989; Sakuraba et al., 2019), and sputtering (Jakosky et al., 1994). However, the source of rich Ne likely supplied major volatile elements (H, C, and N) to form a dense atmosphere. Depending on its amount, such a dense atmosphere might be left for ~100 Myrs timescale. For instance, a recent study (Yoshida and Kuramoto, 2020) suggested that the reducing remnants of Mars' primordial atmosphere, if existed, may contribute to warm early Mars (Ramirez et al., 2014; Ramirez, 2017; Wordsworth et al., 2017) and to form organic matters found to be preserved at Gale crater (Eigenbrode et al., 2018). In contrast, if the abundant Ne was sourced by chondritic or cometary matters, bulk Mars and, consequently, its early atmosphere could be more oxidizing. Secular volcanic degassing of these volatile elements once trapped in the solidified mantle would have also influenced the evolution of early Mars. Thus, unveiling the origin of abundant Ne in Mars' mantle is critical for understanding its early surface environment.

5.4. Earth vs. Mars

Comparing mantle Ne abundances and isotopic ratios between Earth and Mars (Section 2.5) provides several implications for terrestrial planet formation. Substituting Earth's mantle Ne abundance into Eq. (11) results in the lower limit of required Ne partial pressure in the magma ocean stage to be ≃2 Pa. In contrast to Mars, the estimate shows a good match with Ne partial pressure of the current atmosphere (1.8 Pa, Catling and Kasting, 2017). Late processing such as hydrodynamic escape (Hunten et al., 1987; Pepin, 1991; Dauphas, 2003) and impact erosion and replenishment (Marty and Meibom, 2007; Sakuraba et al., 2019) likely influenced Earth's atmospheric Ne content. Moreover, the Earth's primitive mantle could possess more Ne than today's. For example, Earth's depleted mantle has $\simeq 1 \times 10^{-13}$ g/g (Moreira and Kurz, 2013; Marty, 2012), and it has been proposed to be 100 times higher in the beginning (Jaupart et al., 2017). Thus, the consistency of partitioning model for Earth might be a coincidence. However, it emphasizes that Mars' mantle Ne content requires an explanation.

$^{20}Ne/^{22}Ne$ ratio in the Martian mantle is unknown. The ratio in Earth's deep mantle is close to the solar value and suggests the solar nebula origin (Williams and Mukhopadhyay, 2019), while the solar-wind-implanted dust has also been proposed as the origin of Ne (Moreira and Charnoz, 2016). In the solar nebula origin scenario, Earth's accretion timescale longer than that of Mars (Kleine et al., 2009; Dauphas and Pourmand, 2011) as well as the larger mass can result in the different amount of nebula gas capture (Section 4.1). In the case of the solar-wind-implanted dust, there is no reason to expect that Mars preferentially accreted this component compared to Earth. Multiple degassing events followed by atmospheric loss possibly due to giant impacts on Earth (Tucker and Mukhopadhyay, 2014) may lead to the difference to Mars.

6. Conclusions

Ne abundance in the Martian atmosphere was estimated from in situ measurements with Viking landers to be 1–6 ppm. Combining this abundance to the results of numerical modeling validated by the recent upper atmospheric measurements with MAVEN, we estimated the sputtering loss rate and the lifetime of Ne in Martian atmosphere to be $0.7–10 \times 10^{20}$ s^{-1} and $0.6–1 \times 10^{8}$ years, respectively. The short lifetime implies recent or ongoing supply to the atmosphere, but accretion of asteroids, comets, and IDPs and cosmogenic production were found to be insufficient to balance the loss. Thus, we proposed that the presence of atmospheric Ne is evidence of recent or ongoing volcanism on Mars. Ne abundance in the mantle, estimated by using photographic estimate of the magma production rate, is $>0.5–8 \times 10^{-11}$ g/g, which is >5–80 times greater than that in current Earth's mantle. Furthermore, considering dissolution equilibrium between the molten mantle and the overlying atmosphere in the magma ocean stage showed that >300 times more Ne is required to put the estimated Ne abundance into the mantle.

Several possible origins of Martian mantle Ne was discussed. We showed that the solar nebula gas capture under typical conditions is insufficient to explain the abundant Ne in the mantle. Mixing of a degassed component and completion of accretion prior to the nebula gas dissipation were proposed for efficient capture of the nebula gas. On the other hand, Ne can be supplied by chondrites, comets, and solar-wind-implanted dust. These possible Ne sources constrain Mars' accretion history and would have also supplied other highly volatile elements such as H, C, N, and S. Secular degassing from such a volatile-rich mantle has likely affected Mars' climate evolution. Finally, a simple relation between atmospheric and mantle $^{20}Ne/^{22}Ne$ ratios were provided to constrain the origin of mantle Ne by measurements of atmospheric $^{20}Ne/^{22}Ne$ ratio with a future Mars exploration mission or with Mars Sample Return.

CRediT authorship contribution statement

Hiroyuki Kurokawa: Designed the project, Wrote the manuscript, Performed analytic calculations. **Yayoi N. Miura:** Designed the project, Wrote the manuscript. **Seiji Sugita:** Designed the project, Wrote the manuscript. **Yuichiro Cho:** Designed the project, Wrote the manuscript. **François Leblanc:** Designed the project, Wrote the manuscript. **Naoki Terada:** Designed the project, Wrote the manuscript. **Hiromu Nakagawa:** Designed the project, Wrote the manuscript.

Data availability

All data used in this study are given in the main text. Analytic calculations to support the figures are all presented in the main text and an Appendix.

Acknowledgments

We thank Bruce Jakosky and an anonymous reviewer for constructive comments. This study was supported by JSPS KAKENHI, Japan Grant numbers 17H01175, 17H06457, 18K13602, 19H01960, 19H05072, 20KK0080, 21H04514, and 21K13976 and JSPS Core-to-Core program "International Network of Planetary Sciences".

Appendix. Analytical solution for the trapped Ne mass in the mantle

Here we consider partitioning of Ne between the atmosphere, magma ocean, and solidified mantle, and derive an analytical solution for the Ne mass in the mantle at the time when bottom-up mantle

solidification is completed. The mass-balance equations for Ne and mantle are given by,

$$M_{\mathrm{Ne,tot}} = M_{\mathrm{Ne,atm}} + M_{\mathrm{Ne,mo}} + M_{\mathrm{Ne,sm}}, \tag{A.1}$$

and,

$$M_{\mathrm{mantle}} = M_{\mathrm{mo}} + M_{\mathrm{sm}}. \tag{A.2}$$

Combining Eq. (8), (A.1), and (A.2), we obtain,

$$\frac{dM_{\mathrm{Ne,sm}}}{M_{\mathrm{Ne,tot}} - M_{\mathrm{Ne,sm}}} = \frac{F_{\mathrm{tl}} dM_{\mathrm{sm}}}{m_{\mathrm{Ne}} A/\overline{mg} S_{\mathrm{Ne}} + M_{\mathrm{mantle}} - M_{\mathrm{sm}}}. \tag{A.3}$$

Integrating Eq. (A.3) leads to Eq. (9).

References

Atreya, S.K., Trainer, M.G., Franz, H.B., Wong, M.H., Manning, H.L.K., Malespin, C.A., Mahaffy, P.R., Conrad, P.G., Brunner, A.E., Leshin, L.A., et al., 2013. Primordial argon isotope fractionation in the atmosphere of mars measured by the SAM instrument on curiosity and implications for atmospheric loss. Geophys. Res. Lett. 40 (21), 5605–5609.

Balsiger, H., Altwegg, K., Bochsler, P., Eberhardt, P., Fischer, J., Graf, S., Jäckel, A., Kopp, E., Langer, U., Mildner, M., Müller, J., Riesen, T., Rubin, M., Scherer, S., Wurz, P., Wüthrich, S., Arijs, E., Delanoye, S., de Keyser, J., Neefs, E., Nevejans, D., Rème, H., Aoustin, C., Mazelle, C., Médale, J.-L., Sauvaud, J., Berthelier, J.-J., Bertaux, J.-L., Duvet, L., Illiano, J., Fuselier, S., Ghielmetti, A., Magoncelli, T., Shelley, E., Korth, A., Heerlein, K., Lauche, H., Livi, S., Loose, A., Mall, U., Wilken, B., Gliem, F., Fiethe, B., Gombosi, T., Block, B., Carignan, G., Fisk, L., Waite, J., Young, D., Wollnik, H., 2007. ROSINA – Rosetta orbiter spectrometer for ion and neutral analysis. Space Sci. Rev. 128, 745–801.

Beaty, D.W., Grady, M.M., McSween, H.Y., Sefton-Nash, E., Carrier, B.L., Altieri, F., Amelin, Y., Ammannito, E., Anand, M., Benning, L.G., et al., 2019. The potential science and engineering value of samples delivered to earth by mars sample return: International MSR objectives and samples team (iMOST). Meteorit. Planet. Sci. 54, S3–S152.

Bekaert, D.V., Turner, S.J., Broadley, M.W., Barnes, J.D., Halldórsson, S.A., Labidi, J., Wade, J., Walowski, K.J., Barry, P.H., 2020. Subduction-driven volatile recycling: A global mass balance. Ann. Rev. Earth Planet. Sci. 49.

Bierson, C.J., Phillips, R.J., Smith, I.B., Wood, S.E., Putzig, N.E., Nunes, D., Byrne, S., 2016. Stratigraphy and evolution of the buried CO_2 deposit in the Martian south polar cap. Geophys. Res. Lett. 43 (9), 4172–4179.

Blanchard, W.R., McCarthy, P.J., Dylla, H.F., LaMarche, P.H., Simpkins, J.E., 1986. Long-term changes in the sensitivity of quadrupole mass spectrometers. J. Vac. Sci. Technol. 4, 1715–1719.

Borg, L.E., Draper, D.S., 2003. A petrogenetic model for the origin and compositional variation of the martian basaltic meteorites. Meteorit. Planet. Sci. 38 (12), 1713–1731.

Borin, P., Cremonese, G., Marzari, F., Lucchetti, A., 2017. Asteroidal and cometary dust flux in the inner solar system. Astron. Astrophys. 605, A94.

Busemann, H., Baur, H., Wieler, R., 2000. Primordial noble gases in "phase Q" in carbonaceous and ordinary chondrites studied by closed-system stepped etching. Meteorit. Planet. Sci. 35 (5), 949–973.

Catling, D.C., Kasting, J.F., 2017. Atmospheric Evolution on Inhabited and Lifeless Worlds. Cambridge University Press.

Conrad, P.G., Malespin, C.A., Franz, H.B., Pepin, R.O., Trainer, M.G., Schwenzer, S.P., Atreya, S.K., Freissinet, C., Jones, J.H., Manning, H., et al., 2016. In situ measurement of atmospheric krypton and xenon on mars with mars science laboratory. Earth Planet. Sci. Lett. 454, 1–9.

Craddock, R.A., Greeley, R., 2009. Minimum estimates of the amount and timing of gases released into the Martian atmosphere from volcanic eruptions. Icarus 204 (2), 512–526.

Crismani, M.M.J., Schneider, N.M., Plane, J.M.C., Evans, J.S., Jain, S.K., Chaffin, M.S., Carrillo-Sanchez, J.D., Deighan, J.I., Yelle, R.V., Stewart, A.I.F., et al., 2017. Detection of a persistent meteoric metal layer in the Martian atmosphere. Nat. Geosci. 10 (6), 401–404.

Dauphas, N., 2003. The dual origin of the terrestrial atmosphere. Icarus 165 (2), 326–339.

Dauphas, N., Pourmand, A., 2011. Hf–w–th evidence for rapid growth of Mars and its status as a planetary embryo. Nature 473 (7348), 489–492.

Doi, K., Kataoka, A., 2021. Estimate on dust scale height from the ALMA dust continuum image of the HD 163296 protoplanetary disk. Astrophys. J. 912 (2), 164.

Dullemond, C.P., Birnstiel, T., Huang, J., Kurtovic, N.T., Andrews, S.M., Guzmán, V.V., Pérez, L.M., Isella, A., Zhu, Z., Benisty, M., et al., 2018. The disk substructures at high angular resolution project (DSHARP). VI. Dust trapping in thin-ringed protoplanetary disks. Astrophys. J. Lett. 869 (2), L46.

Eigenbrode, J.L., Summons, R.E., Steele, A., Freissinet, C., Millan, M., Navarro-González, R., Sutter, B., McAdam, A.C., Franz, H.B., Glavin, D.P., et al., 2018. Organic matter preserved in 3-billion-year-old mudstones at Gale crater, Mars. Science 360 (6393), 1096–1101.

Elkins-Tanton, L.T., 2008. Linked magma ocean solidification and atmospheric growth for Earth and Mars. Earth Planet. Sci. Lett. 271 (1–4), 181–191.

Farley, K.A., Malespin, C., Mahaffy, P., Grotzinger, J.P., Vasconcelos, P.M., Milliken, R.E., Malin, M., Edgett, K.S., Pavlov, A.A., Hurowitz, J.A., et al., 2014. In situ radiometric and exposure age dating of the martian surface. Science 343 (6169).

Filiberto, J., Baratoux, D., Beaty, D., Breuer, D., Farcy, B.J., Grott, M., Jones, J.H., Kiefer, W.S., Mane, P., McCubbin, F.M., et al., 2016. A review of volatiles in the martian interior. Meteorit. Planet. Sci. 51 (11), 1935–1958.

Flynn, G.J., 1997. The contribution by interplanetary dust to noble gases in the atmosphere of mars. J. Geophys. Res. Planets 102 (E4), 9175–9182.

Frantseva, K., Mueller, M., ten Kate, I.L., van der Tak, F.F.S., Greenstreet, S., 2018. Delivery of organics to mars through asteroid and comet impacts. Icarus 309, 125–133.

Franz, H.B., Trainer, M.G., Malespin, C.A., Mahaffy, P.R., Atreya, S.K., Becker, R.H., Benna, M., Conrad, P.G., Eigenbrode, J.L., 2017. Initial SAM calibration gas experiments on mars: Quadrupole mass spectrometer results and implications. Planet. Space Sci. 138, 44–54.

Füri, E., Marty, B., 2015. Nitrogen isotope variations in the solar system. Nat. Geosci. 8 (7), 515–522.

Garrison, D.H., Bogard, D.D., 1998. Isotopic composition of trapped and cosmogenic noble gases in several martian meteorites. Meteorit. Planet. Sci. 33 (4), 721–736.

Genda, H., Abe, Y., 2005. Enhanced atmospheric loss on protoplanets at the giant impact phase in the presence of oceans. Nature 433 (7028), 842–844.

Genda, H., Ikoma, M., 2008. Origin of the ocean on the earth: early evolution of water D/H in a hydrogen-rich atmosphere. Icarus 194 (1), 42–52.

Greeley, R., Schneid, B.D., 1991. Magma generation on mars: Amounts, rates, and comparisons with Earth, Moon, and Venus. Science 254 (5034), 996–998.

Grott, M., Baratoux, D., Hauber, E., Sautter, V., Mustard, J., Gasnault, O., Ruff, S.W., Karato, S.I., Debaille, V., Knapmeyer, M., et al., 2013. Long-term evolution of the Martian crust-mantle system. Space Sci. Rev. 174 (1–4), 49–111.

Guillot, T., Ida, S., Ormel, C.W., 2014. On the filtering and processing of dust by planetesimals-I. Derivation of collision probabilities for non-drifting planetesimals. Astron. Astrophys. 572, A72.

Halevy, I., Zuber, M.T., Schrag, D.P., 2007. A sulfur dioxide climate feedback on early Mars. Science 318 (5858), 1903–1907.

Hallis, L.J., Huss, G.R., Nagashima, K., Taylor, G.J., Halldórsson, S.A., Hilton, D.R., Mottl, M.J., Meech, K.J., 2015. Evidence for primordial water in Earth's deep mantle. Science 350 (6262), 795–797.

Hallis, L., Taylor, G., Nagashima, K., Huss, G., 2012. Magmatic water in the Martian meteorite Nakhla. Earth Planet. Sci. Lett. 359, 84–92.

Hartmann, W.K., Neukum, G., 2001. Cratering chronology and the evolution of mars. In: Chronology and Evolution of Mars. Springer, pp. 165–194.

Hauber, E., Brož, P., Jagert, F., Jodłowski, P., Platz, T., 2011. Very recent and wide-spread basaltic volcanism on mars. Geophys. Res. Lett. 38 (10).

Hayashi, C., Nakazawa, K., Mizuno, H., 1979. Earth's melting due to the blanketing effect of the primordial dense atmosphere. Earth Planet. Sci. Lett. 43 (1), 22–28.

Heber, V.S., Baur, H., Bochsler, P., McKeegan, K.D., Neugebauer, M., Reisenfeld, D.B., Wieler, R., Wiens, R.C., 2012. Isotopic mass fractionation of solar wind: Evidence from fast and slow solar wind collected by the genesis mission. Astrophys. J. 759 (2), 121.

Heber, V.S., Brooker, R.A., Kelley, S.P., Wood, B.J., 2007. Crystal–melt partitioning of noble gases (helium, neon, argon, krypton, and xenon) for olivine and clinopyroxene. Geochim. Cosmochim. Acta 71 (4), 1041–1061.

Hier-Majumder, S., Hirschmann, M.M., 2017. The origin of volatiles in the earth's mantle. Geochem Geophys Geosyst. 18 (8), 3078–3092.

Hirschmann, M.M., 2016. Constraints on the early delivery and fractionation of earth's major volatiles from C/H, C/N, and C/S ratios. Am. Mineral. 101 (3), 540–553.

Horvath, D.G., Moitra, P., Hamilton, C.W., Craddock, R.A., Andrews-Hanna, J.C., 2021. Evidence for geologically recent explosive volcanism in Elysium Planitia, Mars. Icarus 365, 114499.

Hu, R., Kass, D.M., Ehlmann, B.L., Yung, Y.L., 2015. Tracing the fate of carbon and the atmospheric evolution of mars. Nature Commun. 6 (1), 1–9.

Hunten, D.M., Pepin, R.O., Walker, J.C., 1987. Mass fractionation in hydrodynamic escape. Icarus 69 (3), 532–549.

Hutchins, K.S., Jakosky, B.M., Luhmann, J.G., 1997. Impact of a paleomagnetic field on sputtering loss of martian atmospheric argon and neon. J. Geophys. Res. Planets 102 (E4), 9183–9189.

Iacono-Marziano, G., Paonita, A., Rizzo, A., Scaillet, B., Gaillard, F., 2010. Noble gas solubilities in silicate melts: new experimental results and a comprehensive model of the effects of liquid composition, temperature and pressure. Chem. Geol. 279 (3–4), 145–157.

Ikoma, M., Genda, H., 2006. Constraints on the mass of a habitable planet with water of nebular origin. Astrophys. J. 648 (1), 696.

Jakosky, B.M., 2019. The CO_2 inventory on mars. Planet. Space Sci. 175, 52–59.

Jakosky, B., Brain, D., Chaffin, M., Curry, S., Deighan, J., Grebowsky, J., Halekas, J., Leblanc, F., Lillis, R., Luhmann, J., et al., 2018. Loss of the martian atmosphere to space: Present-day loss rates determined from MAVEN observations and integrated loss through time. Icarus 315, 146–157.

Jakosky, B.M., Henderson, B.G., Mellon, M.T., 1995. Chaotic obliquity and the nature of the Martian climate. J. Geophys. Res. Planets 100 (E1), 1579–1584.

Jakosky, B.M., Pepin, R.O., Johnson, R.E., Fox, J.L., 1994. Mars atmospheric loss and isotopic fractionation by solar-wind-induced sputtering and photochemical escape. Icarus 111 (2), 271–288.

Jakosky, B.M., Slipski, M., Benna, M., Mahaffy, P., Elrod, M., Yelle, R., Stone, S., Alsaeed, N., 2017. Mars' atmospheric history derived from upper-atmosphere measurements of $^{38}Ar/^{36}Ar$. Science 355 (6332), 1408–1410.

Jaupart, E., Charnoz, S., Moreira, M., 2017. Primordial atmosphere incorporation in planetary embryos and the origin of Neon in terrestrial planets. Icarus 293, 199–205.

Johnson, R., Schnellenberger, D., Wong, M., 2000. The sputtering of an oxygen thermosphere by energetic O^+. J. Geophys. Res. Planets 105 (E1), 1659–1670.

Kataoka, A., Muto, T., Momose, M., Tsukagoshi, T., Dullemond, C.P., 2016. Grain size constraints on HL tau with polarization signature. Astrophys. J. 820 (1), 54.

Kleine, T., Touboul, M., Bourdon, B., Nimmo, F., Mezger, K., Palme, H., Jacobsen, S.B., Yin, Q.-Z., Halliday, A.N., 2009. Hf–W chronology of the accretion and early evolution of asteroids and terrestrial planets. Geochim. Cosmochim. Acta 73 (17), 5150–5188.

Kobayashi, H., Dauphas, N., 2013. Small planetesimals in a massive disk formed mars. Icarus 225 (1), 122–130.

Krasnopolsky, V.A., Gladstone, G.R., 2005. Helium on Mars and Venus: EUVE observations and modeling. Icarus 176 (2), 395–407.

Kurokawa, H., Kurosawa, K., Usui, T., 2018. A lower limit of atmospheric pressure on early mars inferred from nitrogen and argon isotopic compositions. Icarus 299, 443–459.

Kurokawa, H., Sato, M., Ushioda, M., Matsuyama, T., Moriwaki, R., Dohm, J.M., Usui, T., 2014. Evolution of water reservoirs on Mars: Constraints from hydrogen isotopes in martian meteorites. Earth Planet. Sci. Lett. 394, 179–185.

Kurokawa, H., Tanigawa, T., 2018. Suppression of atmospheric recycling of planets embedded in a protoplanetary disc by buoyancy barrier. Mon. Not. R. Astron. Soc. 479 (1), 635–648.

Kurokawa, H., Usui, T., Sato, M., 2016. Interactive evolution of multiple water-ice reservoirs on mars: Insights from hydrogen isotope compositions. Geochem. J. 50 (1), 67–79.

Kuwahara, A., Kurokawa, H., 2020a. Influences of protoplanet-induced three-dimensional gas flow on pebble accretion-I. Shear regime. Astron. Astrophys. 633, A81.

Kuwahara, A., Kurokawa, H., 2020b. Influences of protoplanet-induced three-dimensional gas flow on pebble accretion-II. Headwind regime. Astron. Astrophys. 643, A21.

Kuwahara, A., Kurokawa, H., Ida, S., 2019. Gas flow around a planet embedded in a protoplanetary disc - dependence on planetary mass. Astron. Astrophys. 623, A179.

Lal, D., 1993. Cosmogenic and nucleogenic isotopic changes in mars: Their rates and implications to the evolutionary history of Martian surface. Geochim. Cosmochim. Acta 57 (19), 4627–4637.

Lambrechts, M., Johansen, A., 2014. Forming the cores of giant planets from the radial pebble flux in protoplanetary discs. Astron. Astrophys. 572, A107.

Lammer, H., Scherf, M., Kurokawa, H., Ueno, Y., Burger, C., Maindl, T., Johnstone, C.P., Leizinger, M., Benedikt, M., Fossati, L., et al., 2020. Loss and fractionation of noble gas isotopes and moderately volatile elements from planetary embryos and early Venus, Earth and Mars. Space Sci. Rev. 216 (4), 1–50.

Laskar, J., Correia, A., Gastineau, M., Joutel, F., Levrard, B., Robutel, P., 2004. Long term evolution and chaotic diffusion of the insolation quantities of Mars. Icarus 170 (2), 343–364.

Leblanc, F., Benna, M., Chaufray, J.-Y., Martinez, A., Lillis, R., Curry, S., Elrod, M., Mahaffy, P., Modolo, R., Luhmann, J., et al., 2019. First in situ evidence of mars nonthermal exosphere. Geophys. Res. Lett. 46 (8), 4144–4150.

Leblanc, F., Chassefière, E., Gillmann, C., Breuer, D., 2012. Mars' atmospheric 40Ar: A tracer for past crustal erosion. Icarus 218 (1), 561–570.

Leblanc, F., Martinez, A., Chaufray, J., Modolo, R., Hara, T., Luhmann, J., Lillis, R., Curry, S., McFadden, J., Halekas, J., et al., 2018. On mars's atmospheric sputtering after MAVEN's first Martian year of measurements. Geophys. Res. Lett. 45 (10), 4685–4691.

Li, Q., Kiefer, W.S., 2007. Mantle convection and magma production on present-day Mars: Effects of temperature-dependent rheology. Geophys. Res. Lett. 34 (16).

Lillis, R.J., Brain, D.A., Bougher, S.W., Leblanc, F., Luhmann, J.G., Jakosky, B.M., Modolo, R., Fox, J., Deighan, J., Fang, X., et al., 2015. Characterizing atmospheric escape from mars today and through time, with MAVEN. Space Sci. Rev. 195 (1), 357–422.

Lodders, K., 2003. Solar system abundances and condensation temperatures of the elements. Astrophys. J. 591 (2), 1220.

Luhmann, J., Johnson, R., Zhang, M., 1992. Evolutionary impact of sputtering of the Martian atmosphere by O+ pickup ions. Geophys. Res. Lett. 19 (21), 2151–2154.

Luhmann, J., Kozyra, J., 1991. Dayside pickup oxygen ion precipitation at Venus and Mars: Spatial distributions, energy deposition and consequences. J. Geophys. Res. Space Phys. 96 (A4), 5457–5467.

Mahaffy, P., Benna, M., King, T., Harpold, D., Arvey, R., Barciniak, M., Bendt, M., Carrigan, D., Errigo, T., Holmes, V., Johnson, C.S., Kellogg, J., Kimvilakani, P., Lefavor, M., Hengemihle, J., Jaeger, F., Lyness, E., Maurer, J., Melak, A., Noreiga, F., Noriega, M., Patel, K., Prats, B., Raaen, E., Tan, F., Weidner, E., Gundersen, C., Battel, S., Block, B., Arnett, K., Miller, R., Cooper, C., Edmonson, C., Nolan, J.T., 2015. The neutral gas and ion mass spectrometer on the mars atmosphere and volatile evolution mission. Space Sci. Rev. 195, 49–73.

Mahaffy, P.R., Webster, C.R., Atreya, S.K., Franz, H., Wong, M., Conrad, P.G., Harpold, D., Jones, J.J., Leshin, L.A., Manning, H., et al., 2013. Abundance and isotopic composition of gases in the Martian atmosphere from the Curiosity rover. Science 341 (6143), 263–266.

Mahaffy, P.R., Webster, C.R., Cabane, M., Conrad, P.G., Coll, P., Atreya, S.K., Arvey, R., Barciniak, M., Benna, M., Bleacher, L., Brinckerhoff, W.B., Eigenbrode, J.L., Carignan, D., Cascia, M., Chalmers, R., Dworkin, J.P., Errigo, T., Everson, P., Franz, H., Farley, R., Feng, S., Frazier, G., Freissinet, C., Glavin, D.P., Harpold, D.N., Hawk, D., Holmes, V., Johnson, C.S., Jones, A., Jordan, P., Kellogg, J., Lewis, J., Lyness, E., Malespi, C.A., Martin, D.K., Maurer, J., McAdam, A.C., McLennan, D., Nolan, T.J., Noriega, M., Pavlov, A.A., Prats, B., Raaen, E., Sheinman, O., Sheppard, D., Smith, J., Stern, J.C., Tan, F., Trainer, M., Ming, D.W., Morris, R., Jones, J., Gundersen, C., Steele, A., Wray, J., Botta, O., Leshin, L., Owen, T., Battel, S., Jakosky, B.M., Manning, H., Squyres, S., González, R.N., McKay, C.P., Raulin, F., Sternberg, R., Buch, A., Sorensen, P., Schoder, R.K., Coscia, D., Szopa, C., Teinturier, S., Baffes, C., Feldman, J.a., Flesch, G., Forouhar, S., Garcia, R., Keymeulen, D., Woodward, S., Block, B.P., Arnett, K., Miller, R., Edmonson, C., Gorevan, S., Mumm, E., 2012. The sample analysis at Mars investigation and instrument suite. Space Sci. Rev. 170, 401–478.

Mai, C., Desch, S.J., Kuiper, R., Marleau, G.-D., Dullemond, C., 2020. The dynamic proto-atmospheres around low-mass planets with eccentric orbits. Astrophys. J. 899 (1), 54.

Manning, C.V., McKay, C.P., Zahnle, K.J., 2006. Thick and thin models of the evolution of carbon dioxide on Mars. Icarus 180 (1), 38–59.

Marchi, S., Walker, R.J., Canup, R.M., 2020. A compositionally heterogeneous Martian mantle due to late accretion. Sci. Adv. 6 (7), eaay2338.

Marty, B., 2012. The origins and concentrations of water, carbon, nitrogen and noble gases on Earth. Earth Planet. Sci. Lett. 313, 56–66.

Marty, B., Meibom, A., 2007. Noble gas signature of the late heavy bombardment in the earth's atmosphere. EEarth 2 (2), 43–49.

Marty, B., Palma, R.L., Pepin, R.O., Zimmermann, L., Schlutter, D.J., Burnard, P.G., Westphal, A.J., Snead, C.J., Bajt, S., Becker, R.H., et al., 2008. Helium and neon abundances and compositions in cometary matter. Science 319 (5859), 75–78.

Mathew, K., Marti, K., 2001. Early evolution of martian volatiles: Nitrogen and noble gas components in ALH84001 and Chassigny. J. Geophys. Res. Planets 106 (E1), 1401–1422.

Mazor, E., Heymann, D., Anders, E., 1970. Noble gases in carbonaceous chondrites. Geochim. Cosmochim. Acta 34 (7), 781–824.

McDonough, W.F., Sun, S.-S., 1995. The composition of the Earth. Chem. Geol. 120 (3–4), 223–253.

Melosh, H., Vickery, A., 1989. Impact erosion of the primordial atmosphere of Mars. Nature 338 (6215), 487–489.

Meshik, A., Hohenberg, C., Pravdivtseva, O., Donald, B., 2012. Measuring the isotopic composition of solar wind noble gases. In: In Exploring the Solar Wind Ed. M. Laser. In Tech., pp. 99–121.

Miura, Y.N., Okuno, M., Cho, Y., Yoshioka, K., Sugita, S., 2020. Ne-Ar separation using a permeable membrane to measure Ne isotopes for future planetary explorations. Planet. Space Sci. 193, 105046.

Mohapatra, R.K., Schwenzer, S.P., Herrmann, S., Murty, S.V.S., Ott, U., Gilmour, J.D., 2009. Noble gases and nitrogen in martian meteorites Dar al Gani 476, Sayh al Uhaymir 005 and Lewis Cliff 88516: EFA and extra neon. Geochim. Cosmochim. Acta 73 (5), 1505–1522.

Moreira, M., Charnoz, S., 2016. The origin of the neon isotopes in chondrites and on earth. Earth Planet. Sci. Lett. 433, 249–256.

Moreira, M.A., Kurz, M.D., 2013. Noble gases as tracers of mantle processes and magmatic degassing. In: The Noble Gases As Geochemical Tracers. Springer, pp. 371–391.

Nakamura, T., Tajika, E., 2003. Climate change of mars-like planets due to obliquity variations: implications for Mars. Geophys. Res. Lett. 30 (13).

Norman, M.D., 1999. The composition and thickness of the crust of mars estimated from rare earth elements and neodymium-isotopic compositions of Martian meteorites. Meteorit. Planet. Sci. 34 (3), 439–449.

Ohashi, S., Kataoka, A., 2019. Radial variations in grain sizes and dust scale heights in the protoplanetary disk around HD 163296 revealed by ALMA polarization observations. Astrophys. J. 886 (2), 103.

Okuzumi, S., Tazaki, R., 2019. Nonsticky ice at the origin of the uniformly polarized submillimeter emission from the HL tau disk. Astrophys. J. 878 (2), 132.

Olson, P., Sharp, Z.D., 2018. Hydrogen and helium ingassing during terrestrial planet accretion. Earth Planet. Sci. Lett. 498, 418–426.

Olson, P.L., Sharp, Z.D., 2019. Nebular atmosphere to magma ocean: A model for volatile capture during earth accretion. Phys. Earth Planet. Inter. 294, 106294.

O'Neill, C., Lenardic, A., Jellinek, A., Kiefer, W., 2007. Melt propagation and volcanism in mantle convection simulations, with applications for martian volcanic and atmospheric evolution. J. Geophys. Res. Planets 112 (E7).

Ormel, C., Klahr, H., 2010. The effect of gas drag on the growth of protoplanets-analytical expressions for the accretion of small bodies in laminar disks. Astron. Astrophys. 520, A43.
Ormel, C.W., Shi, J.-M., Kuiper, R., 2015. Hydrodynamics of embedded planets' first atmospheres–II. A rapid recycling of atmospheric gas. Mon. Not. R. Astron. Soc. 447 (4), 3512–3525.
Ott, U., 1988. Noble gases in SNC meteorites: Shergotty, Nakhla, Chassigny. Geochim. Cosmochim. Acta 52 (7), 1937–1948.
Owen, T., Biemann, K., Rushneck, D., Biller, J., Howarth, D., Lafleur, A., 1977. The composition of the atmosphere at the surface of Mars. J. Geophys. Res. 82 (28), 4635–4639.
Palma, R.L., Pepin, R.O., Westphal, A.J., Füri, E., Schlutter, D.J., Gainsforth, Z.S., Frank, D.R., 2019. Helium and neon in comet 81p/wild 2 samples from the NASA Stardust mission. Meteorit. Planet. Sci. 54 (1), 3–53.
Park, J., Nagao, K., 2006. New insights on Martian atmospheric neon from Martian meteorite, Dhofar 378. LPI 1110.
Park, J., Nyquist, L., Herzog, G., Nagao, K., Mikouchi, T., Kusakabe, M., 2017. $^{20}Ne/^{22}Ne$ in the martian atmosphere: New evidence from martian meteorites. LPI Abstracts XLVIII 1157.
Pepin, R., 1985. Meteorites: Evidence of martian origins. Nature 317 (6037), 473–474.
Pepin, R.O., 1991. On the origin and early evolution of terrestrial planet atmospheres and meteoritic volatiles. Icarus 92 (1), 2–79.
Pepin, R.O., 1994. Evolution of the martian atmosphere. Icarus 111 (2), 289–304.
Péron, S., Moreira, M., Putlitz, B., Kurz, M., 2017. Solar wind implantation supplied light volatiles during the first stage of earth accretion. Geochem. Perspect. Lett. 3, 151–159.
Phillips, R.J., Davis, B.J., Tanaka, K.L., Byrne, S., Mellon, M.T., Putzig, N.E., Haberle, R.M., Kahre, M.A., Campbell, B.A., Carter, L.M., et al., 2011. Massive CO2 ice deposits sequestered in the south polar layered deposits of Mars. Science 332 (6031), 838–841.
Ramirez, R.M., 2017. A warmer and wetter solution for early Mars and the challenges with transient warming. Icarus 297, 71–82.
Ramirez, R.M., Kopparapu, R., Zugger, M.E., Robinson, T.D., Freedman, R., Kasting, J.F., 2014. Warming early mars with CO_2 and H_2. Nat. Geosci. 7 (1), 59–63.
Ribas, I., Guinan, E.F., Güdel, M., Audard, M., 2005. Evolution of the solar activity over time and effects on planetary atmospheres. I. High-energy irradiances (1-1700 Å). Astrophys. J. 622 (1), 680.
Rivoldini, A., Van Hoolst, T., Verhoeven, O., Mocquet, A., Dehant, V., 2011. Geodesy constraints on the interior structure and composition of Mars. Icarus 213 (2), 451–472.
Robbins, S.J., Di Achille, G., Hynek, B.M., 2011. The volcanic history of mars: High-resolution crater-based studies of the calderas of 20 volcanoes. Icarus 211 (2), 1179–1203.
Rogers, L.A., 2015. Most 1.6 earth-radius planets are not rocky. Astrophys. J. 801 (1), 41.
Rosotti, G.P., Teague, R., Dullemond, C., Booth, R.A., Clarke, C.J., 2020. The efficiency of dust trapping in ringed protoplanetary discs. Mon. Not. R. Astron. Soc. 495 (1), 173–181.
Rubin, M., Altwegg, K., Balsiger, H., Bar-Nun, A., Berthelier, J.-J., Briois, C., Calmonte, U., Combi, M., De Keyser, J., Fiethe, B., et al., 2018. Krypton isotopes and noble gas abundances in the coma of comet 67P/Churyumov-Gerasimenko. Sci. Adv. 4 (7), eaar6297.
Saito, H., Kuramoto, K., 2018. Formation of a hybrid-type proto-atmosphere on Mars accreting in the solar nebula. Mon. Not. R. Astron. Soc. 475 (1), 1274–1287.
Saito, H., Kuramoto, K., 2020. D/h ratio in the interiors of rocky protoplanets accreting in the Solar Nebula. Astrophys. J. 889 (1), 40.
Sakuraba, H., Kurokawa, H., Genda, H., 2019. Impact degassing and atmospheric erosion on Venus, Earth, and Mars during the late accretion. Icarus 317, 48–58.
Sasaki, S., 1999. Presence of a primary solar-type atmosphere around the earth: Evidence of dissolved noble gas. Planet. Space Sci. 47 (12), 1423–1431.
Sasaki, S., Nakazawa, K., 1990. Did a primary solar-type atmosphere exist around the proto-Earth? Icarus 85 (1), 21–42.
Schwenzer, S.P., Herrmann, S., Mohapatra, R.K., Ott, U., 2007. Noble gases in mineral separates from three shergottites: Shergotty, Zagami, and EETA79001. Meteorit. Planet. Sci. 42 (3), 387–412.
Sharp, Z.D., 2017. Nebular ingassing as a source of volatiles to the terrestrial planets. Chem. Geol. 448, 137–150.
Sholes, S.F., Smith, M.L., Claire, M.W., Zahnle, K.J., Catling, D.C., 2017. Anoxic atmospheres on mars driven by volcanism: Implications for past environments and life. Icarus 290, 46–62.
Slipski, M., Jakosky, B.M., 2016. Argon isotopes as tracers for Martian atmospheric loss. Icarus 272, 212–227.
Smith, T., Ranjith, P., He, H., Zhu, R., 2020. Reviewing martian atmospheric noble gas measurements: From Martian Meteorites to Mars missions. Geosciences 10 (11), 439.
Stevenson, D.J., 1982. Formation of the giant planets. Planet. Space Sci. 30 (8), 755–764.
Stone, S.W., Yelle, R.V., Benna, M., Elrod, M.K., Mahaffy, P.R., 2018. Thermal structure of the Martian upper atmosphere from MAVEN NGIMS. J. Geophys. Res. Planets 123 (11), 2842–2867.
Swindle, T.D., 2002. Martian noble gases. Rev. Mineral. Geochem. 47 (1), 171–190.
Swindle, T., Caffee, M., Hohenberg, C., 1986. Xenon and other noble gases in shergottites. Geochim. Cosmochim. Acta 50 (6), 1001–1015.
Terada, N., Kulikov, Y.N., Lammer, H., Lichtenegger, H.I.M., Tanaka, T., Shinagawa, H., Zhang, T., 2009. Atmosphere and water loss from early mars under extreme solar wind and extreme ultraviolet conditions. Astrobiology 9 (1), 55–70.
Tian, F., Claire, M.W., Haqq-Misra, J.D., Smith, M., Crisp, D.C., Catling, D., Zahnle, K., Kasting, J.F., 2010. Photochemical and climate consequences of sulfur outgassing on early mars. Earth Planet. Sci. Lett. 295 (3–4), 412–418.
Trieloff, M., Kunz, J., Clague, D.A., Harrison, D., Allègre, C.J., 2000. The nature of pristine noble gases in mantle plumes. Science 288 (5468), 1036–1038.
Tu, L., Johnstone, C.P., Güdel, M., Lammer, H., 2015. The extreme ultraviolet and X-ray sun in time: High-energy evolutionary tracks of a solar-like star. Astron. Astrophys. 577, L3.
Tucker, J.M., Mukhopadhyay, S., 2014. Evidence for multiple magma ocean outgassing and atmospheric loss episodes from mantle noble gases. Earth Planet. Sci. Lett. 393, 254–265.
Ueda, T., Kataoka, A., Tsukagoshi, T., 2020. Scattering-induced intensity reduction: Large mass content with small grains in the inner region of the TW Hya disk. Astrophys. J. 893 (2), 125.
Usui, T., Alexander, C.M., Wang, J., Simon, J.I., Jones, J.H., 2012. Origin of water and mantle–crust interactions on mars inferred from hydrogen isotopes and volatile element abundances of olivine-hosted melt inclusions of primitive shergottites. Earth Planet. Sci. Lett. 357, 119–129.
Vasconcelos, P.M., Farley, K.A., Malespin, C.A., Mahaffy, P., Ming, D., McLennan, S.M., Hurowitz, J.A., Rice, M.S., 2016. Discordant K-Ar and young exposure dates for the Windjana sandstone, Kimberley, Gale Crater, Mars. J. Geophys. Res. Planets 121 (10), 2176–2192.
Vogt, M., Hopp, J., Gail, H.-P., Ott, U., Trieloff, M., 2019. Acquisition of terrestrial neon during accretion–a mixture of solar wind and planetary components. Geochim. Cosmochim. Acta 264, 141–164.
Weiss, B.P., Bai, X.-N., Fu, R.R., 2021. History of the solar nebula from meteorite paleomagnetism. Sci. Adv. 7 (1), eaba5967.
Wieler, R., 2002. Noble gases in the solar system. Rev. Mineral. Geochem. 47 (1), 21–70.
Wiens, R., Becker, R., Pepin, R., 1986. The case for a martian origin of the shergottites, II. Trapped and indigenous gas components in EETA 79001 glass. Earth Planet. Sci. Lett. 77 (2), 149–158.
Williams, C.D., Mukhopadhyay, S., 2019. Capture of nebular gases during Earth's accretion is preserved in deep-mantle neon. Nature 565 (7737), 78–81.
Wood, B.E., Müller, H.-R., Zank, G.P., Linsky, J.L., 2002. Measured mass-loss rates of solar-like stars as a function of age and activity. Astrophys. J. 574 (1), 412.
Wordsworth, R., Kalugina, Y., Lokshtanov, S., Vigasin, A., Ehlmann, B., Head, J., Sanders, C., Wang, H., 2017. Transient reducing greenhouse warming on early mars. Geophys. Res. Lett. 44 (2), 665–671.
Wu, J., Desch, S.J., Schaefer, L., Elkins-Tanton, L.T., Pahlevan, K., Buseck, P.R., 2018. Origin of earth's water: chondritic inheritance plus nebular ingassing and storage of hydrogen in the core. J. Geophys. Res. Planets 123 (10), 2691–2712.
Yokochi, R., Marty, B., 2004. A determination of the neon isotopic composition of the deep mantle. Earth Planet. Sci. Lett. 225 (1–2), 77–88.
Yoshida, T., Kuramoto, K., 2020. Sluggish hydrodynamic escape of early Martian atmosphere with reduced chemical compositions. Icarus 345, 113740.
Yoshida, N., Nakagawa, H., Terada, N., Evans, J., Schneider, N., Jain, S., Imamura, T., Chaufray, J.-Y., Fujiwara, H., Deighan, J., et al., 2020. Seasonal and latitudinal variations of dayside N_2/CO_2 Ratio in the Martian thermosphere derived from MAVEN IUVS observations. J. Geophys. Res. Planets 125 (12), e2020JE006378.